Non-Markovian dynamics of a nanomechanical resonator measured by a quantum point contact

Po-Wen Chen, Chung-Chin Jian, and Hsi-Sheng Goan*

Department of Physics and Center for Theoretical Sciences, National Taiwan University, Taipei 10617, Taiwan

Center for Quantum Science and Engineering, National Taiwan University, Taipei 10617, Taiwan

(Received 19 April 2010; revised manuscript received 19 November 2010; published 22 March 2011)

We study the dynamics of a nanomechanical resonator (NMR) subject to a measurement by a low-transparency quantum point contact (QPC) or tunnel junction in the non-Markovian domain. We derive the non-Markovian number-resolved (conditional) and unconditional master equations valid to second order in the tunneling Hamiltonian without making the rotating-wave approximation and the Markovian approximation, generally made for systems in quantum optics. Our non-Markovian master equation reduces, in appropriate limits, to various Markovian versions of master equations in the literature. We find considerable difference in dynamics between the non-Markovian case and its Markovian counterparts. We also calculate the time-dependent transport current through the QPC, which contains information about the measured NMR system. We find an extra transient current term proportional to the expectation value of the symmetrized product of the position and momentum operators of the NMR. This extra current term, with a coefficient coming from the combination of the imaginary parts of the QPC reservoir correlation functions, has a substantial contribution to the total transient current in the non-Markovian case, but was generally ignored in the studies of the same problem in the literature. Considering the contribution of this extra term, we show that a significant qualitative and quantitative difference in the total transient current between the non-Markovian and the Markovian wideband-limit cases can be observed. Thus, it may serve as a witness or signature of the non-Markovian features in the coupled NMR-QPC system.

DOI: 10.1103/PhysRevB.83.115439 PACS number(s): 73.23.−b, 85.85.+j, 03.65.Yz, 03.65.Ta

I. INTRODUCTION

Recent advances in nanotechnology have enabled the fabrication of very small quantum electronic devices that incorporate mechanical degrees of freedom, called nanomechanical systems.[1–7] The interplay between electronic and mechanical degrees of freedom has generated interesting dynamical effects.[8–12] These advances have also opened a new avenue to the technology of high-precision displacement measurement using electronic devices, such as quantum dots, single-electron transistors (SET's), or quantum point contacts (QPC's).[12–23] Experiments using SET's and QPC's have demonstrated displacement detections of a nanomechanical resonator (NMR) with sensitivities close to the standard quantum limit.[13–16] Similar problems of a two-level system measured by QPC's or SET's have also attracted much attention[24–34] theoretically and experimentally.

The transport properties in nanostructure electronic devices are often studied theoretically in the wideband limit (WBL) and under the Markovian approximation.[12,17–32] The WBL approximation neglects the important fact that electron tunneling amplitudes and also the electrodes' densities of states are in general energy dependent. The Markovian approximation assumes that the correlation time of the electrons in the electrodes (reservoirs) is much shorter than the typical system response time. These approximations may not be always true in realistic nanostructure devices. Hence, a recent development in quantum nanostructure electronic transport has been devoted to the study of the non-Markovian effects on the electron transport properties, taking into account the energy-dependent spectral density of electrodes.[33,35–44] In this paper, we investigate the dynamics of a NMR subject to a measurement by a low-transparency QPC or a tunnel junction in the non-Markovian domain. This problem has been extensively studied in the literature under various conditions and approximations.[19–23] In Ref. 19 a master equation of the reduced density matrix of a NMR was obtained for zero-temperature QPC reservoirs (electrodes) in the high-bias limit. The master equation presented in Ref. 20 included not only the effect of the QPC reservoirs in the high-bias limit but also the effect of a high-temperature thermal environment on the NMR. The master equation derived in Ref. 21 was claimed to be applicable for a broad range of QPC temperatures and bias voltages and for arbitrary NMR frequencies. However, the results presented in these papers[19–23] were under the Markovian approximation and without consideration of the energy-dependent spectral density of electrodes. In this paper, we take these into account and derive a time-local (time-convolutionless) non-Markovian master equation[43,45–55] that reduces, in appropriate limits, to various Markovian versions of the master equations in Refs. 19–23. We find considerable differences in dynamics between the non-Markovian case and its Markovian counterpart in some parameter regimes. We also calculate the time-dependent transport current through the QPC, which contains information about the measured NMR system. We find an extra transient current term proportional to the expectation value of the symmetrized product of the position and momentum operators of the NMR. This extra current term, with a coefficient coming from the combination of the imaginary parts of the QPC reservoir correlation functions, has a substantial contribution to the total transient current in the non-Markovian case and differs qualitatively and quantitatively from its Markovian WBL counterpart. But it was generally ignored in the studies of the same problem in the literature.[19–23] Considering the contribution of this extra term, we show in this paper that a significant qualitative and quantitative difference in the total transient current between the non-Markovian and the Markovian WBL cases can be observed. Thus, it may serve as a witness or signature of the non-Markovian features in the coupled NMR-QPC system.

The paper is organized as follows. In Sec. II, we describe our NMR-QPC model. In Sec. III, we derive a time-local (time-convolutionless) non-Markovian[43,45–55] number-resolved or n-resolved[20,21,24–27,29,31,32] (conditional) master equation of the density matrix of the NMR subject to a measurement of a QPC detector and the influence of a thermal bath. Our non-Markovian equation is valid for arbitrary bath temperatures, electrode reservoir temperatures, bias voltages, and NMR frequencies as long as the approximation used in our approach, namely, the second-order perturbation in the system-bath and system-reservoir coupling strengths, holds. In Sec. IV, we present the unconditional non-Markovian master equation and show that the unconditional non-Markovian master equation we obtain reduces, in appropriate limits, to various Markovian versions of the master equations in the literature. In Sec. V, we calculate the non-Markovian expectation values of the NMR dynamical variables. The time-dependent transport current through the QPC, which contains information about the measured NMR system, is calculated in Sec. VI. We follow Ref. 21 to categorize the non-Markovian average current into several physically distinct contributions. We find an extra transient current term that has a substantial contribution to the total transient current in the non-Markovian case. Numerical results together with discussions are presented in Sec. VII. A conclusion is given in Sec. VIII.

II. HAMILTONIAN OF THE NMR-QPC MODEL

In this section, we describe the model of a NMR that is subject to a measurement by a low-transparency QPC or electric tunnel junction[18–23] and is under the influence of a thermal environment (see Fig. 1). In this model, the NMR is considered as a quantum harmonic oscillator, and the thermal environment and the QPC electrodes (leads) are treated as an equilibrium bosonic bath and nonequilibrium fermionic reservoirs, respectively. By considering the NMR linearly coupled to the QPC, the Hamiltonian can then be written as

$$H = H_S + H_B + H_I, \tag{1}$$

where

$$H_S = \frac{p^2}{2m} + \frac{1}{2}m\omega_0^2 x^2, \tag{2}$$

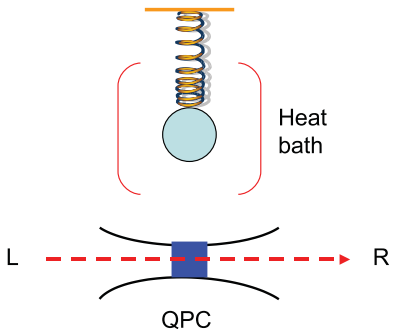

FIG. 1. (Color online) Schematic diagram of a nanomechanical resonator (NMR) coupled to a thermal reservoir and measured by a quantum point contact (QPC) detector.

$$H_B = H_{\text{leads}} + \sum_n \left(\frac{p_n^2}{2m_n} + \frac{1}{2}m_n\omega_n^2 q_n^2\right) \tag{3}$$

with

$$H_{\text{leads}} = \sum_{l=S,D} H_{\text{lead}}^l = \sum_{l=S,D}\sum_k \epsilon_k^l c_{l,k}^\dagger c_{l,k} \tag{4}$$

and

$$H_I = H_{\text{tunneling}} + \sum_n \lambda_n q_n x, \tag{5}$$

with

$$H_{\text{tunneling}} = \sum_{k,q}(T_{kq} + \chi_{kq}x)c_{S,k}^\dagger c_{D,q} + \text{H.c.} \tag{6}$$

Here H_S represents the Hamiltonian of the NMR system, and m and ω_0 are the mass and the (renormalized) natural frequency of the NMR, respectively. H_B represents the Hamiltonian for the left and right leads (reservoirs) of the QPC and the thermal (bosonic) bath. The thermal bath in Eq. (3) consists of a large number of harmonic oscillators with masses m_n and frequencies ω_n, respectively. In Eq. (4), $c_{l,k}$ and ϵ_k^l are, respectively, the fermion (electron) reservoir annihilation operators and energies with wave vector k for the left (source) or right (drain) lead of the QPC. The interaction Hamiltonian H_I, Eq. (5), contains two parts: the first term describes the tunneling Hamiltonian of the electrons through the QPC and the second term describes the interaction between the NMR and the thermal environment. In Eq. (6), the bare tunneling amplitude between respective states with wave vectors k and q in the left and right leads (reservoirs) of the QPC is given by T_{kq}, and H.c. stands for the Hermitian conjugate of the previous term. So the interaction between the NMR and QPC introduces an effective tunneling amplitude[21] from $T_{kq} \to T_{kq} + \chi_{kq}x$ in Eq. (6). The NMR and each of the thermal bath oscillators interact bilinearly through their respective position operators as shown in the last term of Eq. (5), and λ_n is the coupling strength.

III. NUMBER-RESOLVED QUANTUM MASTER EQUATION

Non-Markovian dynamics usually means that the current time evolution of the system state depends on its history, and the memory effects typically enter through integrals over the past state history. However, the non-Markovian system dynamics of some classes of open quantum system models may be summed up and expressed as a time-local, convolutionless form[56] where the dynamics is determined by the system state at the current time t only. This time-local, convolutionless class of open quantum systems may be treated exactly without any approximation. The quantum Brownian motion model or the damped harmonic oscillator bilinearly coupled to a bosonic bath of harmonic oscillators[56–58] is a famous example of this class. The pure-dephasing spin-boson model[59–64] also belongs to this class. The non-Markovian effects in the master equations are taken into account by the time-dependent decoherence, damping, and/or diffusion coefficients instead of convolution memory integrals.

The perturbative non-Markovian open quantum system theory may also be categorized into two classes: the time-nonlocal and the time-local (or time-convolutionless) methods. This has been discussed extensively in the literature.[46–48,51] In the quantum master equation approach, after the Born approximation, the master equation of the reduced density matrix $\rho(t)$ of the system could be an integro-differential equation and thus nonlocal in time. In the interaction picture, the master equation in this case can be written as [48,65,66]

$$\frac{d\tilde{\rho}(t)}{dt} = -\frac{1}{\hbar^2}\mathrm{Tr}_R \int_0^t dt'[\tilde{H}_I(t),[\tilde{H}_I(t'),\tilde{\rho}(t')\otimes R_0]], \quad (7)$$

where $\tilde{\rho}(t)$ is the reduced density matrix of the system and $\tilde{H}_I(t)$ is the system-reservoir interaction Hamiltonian in the interaction picture. In obtaining Eq. (7), the assumption of the initial total density matrix in the uncorrelated (factorized) form of $\tilde{\rho}_T(0) = \tilde{\rho}(0)\otimes R_0$ (with R_0 being the reservoir density matrix) and the assumption that the system-reservoir interaction Hamiltonian satisfies the condition of

$$\mathrm{Tr}_R[\tilde{H}_I(t)R_0] = 0, \quad (8)$$

to eliminate the first-order term in $\tilde{H}_I$ are made. However, it can also be shown that another systematically perturbative non-Markovian master equation that is local in time[43,45–55] can be derived from the time-convolutionless projection operator formalism[45–48] or from the iteration expansion method.[49] Under the similar assumptions of the factorized initial system-reservoir density matrix state and Eq. (8), the second-order time-convolutionless master equation can be obtained as

$$\frac{d\tilde{\rho}(t)}{dt} = -\frac{1}{\hbar^2}\mathrm{Tr}_R \int_0^t dt'[\tilde{H}_I(t),[\tilde{H}_I(t'),\tilde{\rho}(t)\otimes R_0]]. \quad (9)$$

We note here that obtaining the time-convolutionless non-Markovian master equation perturbatively up to only second order in the interaction Hamiltonian is equivalent to replacing $\tilde{\rho}(t')$ with $\tilde{\rho}(t)$ in Eq. (7).[46–49,51] One may be tempted to think that the second-order time-nonlocal master equation (7) is more accurate than the second-order time-local (time-convolutionless) master equation (9) since besides the Born approximation, the (first) Markovian approximation of replacing $\tilde{\rho}(t')$ with $\tilde{\rho}(t)$ in Eq. (7) seems to be an additional approximation made on the time-local master equation. But it has been shown[43,46,48,51] that this may not be the case. In many examples,[43,46,48,51] the time-convolutionless approach works better than the time-nonlocal approach when the exact dynamics is available and is used to test the perturbative non-Markovian theory based on these two approaches. The Markovian approximation that we refer to here corresponds to the (second) Markovian approximation where the bath (reservoir) correlation functions are δ correlated in time. In this (second) Markovian limit, one may change in Eq. (9) the integration variable t' to $\tau = t - t'$ and then extend the upper limit of the time τ integral to infinity (i.e., $t \to \infty$) as the bath correlation functions (kernels) are δ correlated in time and thus sharply peak at the lower limit $\tau = 0$ of the integral. Recently, there are several investigations[67–70] of constructing different measures of non-Markovianity to quantify the degree of non-Markovian behavior of the quantum time evolutions of general systems in contact with an environment. In this paper, we do not concern ourselves with determining the degree of non-Markovian character as investigated in Refs. 67–70. The non-Markovian process here means that we do not make the (second) Markovian approximation of assuming the bath (reservoir) correlation functions being δ correlated in time in Eq. (9) to obtain the second-order time-convolutionless master equation, so the resultant quantum dynamics of the system state is not Markovian. In other words, the influence of the coarse-grained environment causes nonlocal noise correlations and the memory effects of the non-Markovian dynamical process are contained in the *time-dependent* decoherence, damping, and/or diffusion coefficients of the time-convolutionless master equation rather than *time-independent* ones in the Markovian case.

We will derive conditional number-resolved (or n-resolved) and unconditional quantum master equations for the reduced density matrix of the NMR up to second order in the effective tunneling amplitude and in the NMR–thermal-bath coupling strength. The n-resolved master equation[20,21,24–27,29,31,32] describes the dynamics of the reduced NMR system state conditioned on the number n of the electrons that have tunneled through the QPC detector in time interval of $(0,t)$, and is thus ready to be used to calculate the transport properties, such as the transport current. The unconditional master equation can be obtained by summing all possible numbers of electrons n in the right lead (drain) of the QPC. We will present the derivation of the non-Markovian (time-convolutionless form) master equation of the reduced density matrix of the NMR system by considering only the nonequilibrium QPC fermionic reservoirs first, and will include the effect of the equilibrium thermal bosonic bath in the derived master equation later. To proceed with the derivation, it is convenient to go to the interaction picture[48,65] with respect to $H_0 = H_S + H_{\mathrm{leads}}$. The dynamics of the entire system is determined by the time-dependent tunneling Hamiltonian in the interaction picture

$$\tilde{H}_I(t) = \tilde{H}_{\mathrm{tunneling}}(t) = \sum_{k,q}[T_{kq} + \chi_{kq}x(t)] \times e^{i(\epsilon_k^S - \epsilon_q^D)t/\hbar}c_{S,k}^\dagger c_{D,q} + \mathrm{H.c.}, \quad (10)$$

where $x(t) = x\cos(\omega_0 t) + (p/m\omega_0)\sin(\omega_0 t)$. By rewriting

$$x(t) = \left(\frac{x}{2} - i\frac{p}{2m\omega_0}\right)e^{i\omega_0 t} + \left(\frac{x}{2} + i\frac{p}{2m\omega_0}\right)e^{-i\omega_0 t}, \quad (11)$$

the interaction (tunneling) Hamiltonian, Eq. (10), can be written in the form of

$$\tilde{H}_I(t) = \sum_{k,q} S_{kq}(t)F_{kq}^\dagger(t) + S_{kq}^\dagger(t)F_{kq}(t), \quad (12)$$

where

$$F_{kq}(t) = e^{-i(\epsilon_k^S - \epsilon_q^D)t/\hbar}c_{S,k}c_{D,q}^\dagger \quad (13)$$

is the reservoir operator and

$$S_{kq}(t) = [P_1 + e^{i\omega_0 t}P_2 + e^{-i\omega_0 t}P_3] \quad (14)$$

is an operator in a discrete Fourier decomposition[30] acting on the Hilbert space of the NMR system. Introducing the dimensionless characteristic length $x_0 = \sqrt{\hbar/m\omega_0}$ and momentum $p_0 = \sqrt{m\hbar\omega_0}$, we may write

$$P_1 = T_{kq}, \quad (15)$$

$$P_2 = \tilde{\chi}_{kq}\left(\frac{x}{2x_0} - i\frac{p}{2p_0}\right), \tag{16}$$

$$P_3 = \tilde{\chi}_{kq}\left(\frac{x}{2x_0} + i\frac{p}{2p_0}\right), \tag{17}$$

where $\tilde{\chi}_{kq} = \chi_{kq}x_0$ has a dimension the same as T_{kq}. The form of Eq. (14) indicates that there are three different jump processes that involve no excitation, excitation, and relaxation of the energy quanta of the NMR, respectively. P_1 is associated with elastic (no excitation) tunneling of electrons through the QPC junction and P_2 (P_3) is associated with inelastic excitation (relaxation) of electrons tunneling through the QPC with an energy transfer $\hbar\omega_0$. The energy which relaxes (excites) in response is provided by the NMR. By regarding the tunneling Hamiltonian Eq. (12) as a perturbative interaction Hamiltonian, one can see that the first-order term vanishes, i.e., Eq. (8) is satisfied, for the density matrix of the QPC reservoirs (leads) given by $R_0 = \rho^S_{\rm lead} \otimes \rho^D_{\rm lead}$, where

$$\rho^l_{\rm lead} = \frac{e^{-\beta(H^l_{\rm lead} - \mu_l \hat{N}_l)}}{{\rm Tr}_l[e^{-\beta(H^l_{\rm lead} - \mu_l \hat{N}_l)}]}, \qquad l = S, D. \tag{18}$$

Here $\hat{N}_l = \sum_k c^\dagger_{l,k} c_{l,k}$, μ_S and μ_D are the chemical potentials which determine the applied QPC bias voltage, $eV = \mu_S - \mu_D$, and $\beta = 1/(k_B T)$ is the inverse temperature. One may then obtain the second-order (Born approximation) time-convolutionless non-Markovian master equation for the reduced density matrix of the NMR system by substituting Eq. (12) into Eq. (9). However, in order to make contact of the NMR system with the QPC detector output current, it will be convenient to obtain an n-resolved master equation.[20,21,24–27,29,31,32] The rotating-wave approximation and Markovian approximation are known to be quite good approximations for systems in quantum optics. The rotating-wave approximation is a good approximation provided that the strength of the dissipative corrections or the relaxation rate, denoted generically as γ_R, is small compared to the minimum nonzero system frequency difference (energy difference/$\hbar$) involved in the problem. In the present case, this implies that the generic rate γ_R in the conditional n-resolved and unconditional master equations should satisfy the condition of $\gamma_R \ll \omega_0$. The relevant physical condition for the Markovian approximation is that the bath correlation time is very small compared to the typical system response time. But since the (renormalized) resonant frequency ω_0 of a NMR is typically in the range of a few hundred kilohertz to a few gigahertz, which is much smaller than the typical optical frequency of 10^{15} Hz and since the reservoir correlation time in solid-state devices may not be much shorter than the typical system response time, we will not make the Markovian approximation and the *pretrace* and *post-trace* rotating-wave approximations[71–73] in our derivation of the master equation. By first identifying the jump operator terms and partially taking trace over the microscopic degrees of freedom of the QPC reservoirs but keeping track of the number n of electrons that have tunneled through the QPC detector during the time period $(0,t)$, and then changing from the interaction picture to the Schrödinger picture, we can obtain from Eqs. (9) and (12) the time-convolutionless non-Markovian n-resolved (conditional) master equation as

$$\begin{aligned}\dot{\rho}^{(n)}_R(t) = {}& \frac{1}{i\hbar}[H_{\rm sys}, \rho^{(n)}_R(t)] - \frac{1}{\hbar^2}\int_0^t dt_1 \sum_{k,q;k',q'} \Big[F^s_{kq;k'q'}(t,t_1)\big(S_{kq}(t)S^\dagger_{k'q'}(t_1)\rho^{(n)}_R(t) - S^\dagger_{k'q'}(t_1)\rho^{(n+1)}_R(t)S_{kq}(t) \\ & - S_{kq}(t)\rho^{(n-1)}_R(t)S^\dagger_{k'q'}(t_1) + \rho^{(n)}_R(t)S^\dagger_{k'q'}(t_1)S_{kq}(t)\big) - F^a_{kq;k'q'}(t,t_1)\big(S_{kq}(t)S^\dagger_{k'q'}(t_1)\rho^{(n)}_R(t) - S^\dagger_{k'q'}(t_1)\rho^{(n+1)}_R(t)S_{kq}(t) \\ & + S_{kq}(t)\rho^{(n-1)}_R(t)S^\dagger_{k'q'}(t_1) - \rho^{(n)}_R(t)S^\dagger_{k'q'}(t_1)S_{kq}(t)\big) + {\rm H.c.}\Big] + \mathcal{L}_{\rm damp}\big[\rho^{(n)}_R(t)\big],\end{aligned} \tag{19}$$

where we have also included the intrinsic dissipation effect of the NMR induced by interacting with a non-Markovian thermal bosonic environment in the last term of Eq. (19). The mode-dependent symmetric and antisymmetric two-time reservoir correlation functions, $F^s_{k,q;k',q'}(t,t_1)$ and $F^a_{k,q;k',q'}(t,t_1)$ in Eq. (19), are respectively,

$$\begin{aligned}F^s_{kq;k'q'}(t,t_1) &\equiv \tfrac{1}{2}\langle\{F^\dagger_{k,q}(t), F_{k',q'}(t_1)\}\rangle \\ &= \tfrac{1}{2}\{N_{Sk}(1-N_{Dq}) + (1-N_{Sk})N_{Dq}\} \\ &\quad \times e^{i(\epsilon^S_k - \epsilon^D_q)(t-t_1)/\hbar}\delta_{k,q;k',q'}\end{aligned} \tag{20}$$

and

$$\begin{aligned}F^a_{k,q;k',q'}(t,t_1) &\equiv \tfrac{1}{2}\langle[F^\dagger_{k,q}(t), F_{k',q'}(t_1)]\rangle \\ &= \tfrac{1}{2}\{N_{Sk}(1-N_{Dq}) - (1-N_{Sk})N_{Dq}\} \\ &\quad \times e^{i(\epsilon^S_k - \epsilon^D_q)(t-t_1)/\hbar}\delta_{k,q;k',q'}.\end{aligned} \tag{21}$$

Here the notation $\langle\cdots\rangle$ indicates the expectation value over the initial density matrix of the reservoirs and consequently $F^s_{k,q;k',q'}(t,t_1)$ and $F^a_{k,q;k',q'}(t,t_1)$ are given by the combination of the Fermi distribution functions $N_{Sk} = [e^{\beta(\epsilon^S_k - \mu_S)} + 1]^{-1}$ and $N_{Dq} = [e^{\beta(\epsilon^D_q - \mu_D)} + 1]^{-1}$ of the left (source) and right (drain) reservoirs of the QPC.[28,29,31,32] By taking into account relevant tunneling amplitudes and summing over the wave vectors of the QPC reservoirs, the structure of the influence of the QPC reservoirs on the dynamics of the NMR system is then characterized by the symmetric and antisymmetric two-time reservoir correlation kernels $\sum_{k,q,k',q'} A^\dagger_{k,q}B_{k,q}F^s_{k,q;k',q'}(t,t_1)$ and $\sum_{k,q,k',q'} A^\dagger_{k,q}B_{k,q}F^a_{k,q;k',q'}(t,t_1)$, where the value of $A_{k,q}$ and $B_{k,q}$ could be any one of the tunneling amplitudes $T_{k,q}$ and $\tilde{\chi}_{k,q} = \chi_{k,q}x_0$. In the continuous limit, the summation of the QPC reservoir modes can be replaced by the continuous integrations, $\sum_k \sum_q \to \int\int d\epsilon^S_k d\epsilon^D_q\, g_L(\epsilon^S_k) g_R(\epsilon^D_q)$, where the energy-dependent densities of states $g_S(\epsilon^S_k)$ and $g_D(\epsilon^D_q)$ are introduced for left and right QPC electron reservoirs,

respectively. In principle, the tunneling amplitudes $T_{k,q} = T(\epsilon_k^S,\epsilon_q^D)$ and $\tilde{\chi}_{k,q} = \tilde{\chi}(\epsilon_k^S,\epsilon_q^D)$ are also energy dependent. We may deal with any realistic energy function form of the densities of states and tunneling amplitudes to take into account the memory effect of the QPC reservoir on the electron transport and the NMR system in our non-Markovian treatment. For simplicity, we follow several non-Markovian electron transport studies[33,36–39,41–43,74,75] by considering a spectral density with energy-dependent densities of states and tunneling amplitudes absorbed in a Lorentzian form as

$$J_{A,B}(\epsilon_k^S,\epsilon_q^D) = A^\dagger(\epsilon_k^S,\epsilon_q^D)B(\epsilon_k^S,\epsilon_q^D)g_L(\epsilon_k^S)g_R(\epsilon_q^D) = \frac{A_{00}^\dagger B_{00} g_L^0 g_R^0 \Lambda_e^2}{(\epsilon_k^S - \epsilon_q^D - E_i)^2 + \Lambda_e^2}, \tag{22}$$

where the cutoff energy Λ_e characterizes the width of the Lorentzian energy-dependent distribution, the parameter E_i denotes the effect of the variation of the QPC junction barrier potential[33] due to the interaction with the NMR, A_{00}, B_{00}, g_L^0, and g_R^0 are energy-independent tunneling amplitudes and densities of states near the average chemical potential. Physically, this spectral density of Eq. (22) means that given an electron state with a fixed energy ϵ_k^S in the left lead, the electron can tunnel into the electron energy states of the right lead with a central energy at $\epsilon_q^D + E_i$ and a Lorentzian width Λ_e. In the limit of $\Lambda_e \to 0$ and in the absence of the interaction with the NMR (i.e., $E_i = 0$), the QPC spectral density Eq. (22) is proportional to $\delta(\epsilon_k^S - \epsilon_q^D)$ which represents the resonant tunneling process. In the opposite case of the cutoff energy $\Lambda_e \to \infty$, the QPC spectral density Eq. (22) becomes energy independent and reduces to the constant WBL spectral density used in the literature. The average (effective) zero-temperature electron tunneling conductances (G/e^2) through the QPC barrier in the WBL can be written as $(2\pi/\hbar)A_{00}^\dagger B_{00} g_L^0 g_R^0$. Compared with the energy-dependent spectral density, the WBL one that assumes all electron states in the left reservoir having equal likelihood to tunnel to all the electron states in the right reservoir regardless of their energies may not be a very good physical approximation after all.

We note that the dynamical behaviors of the NMR-QPC system are sensitive to the actual energy dependence and the bandwidth of the QPC spectral density (which may be different from the simple Lorentzian form considered here). The realistic energy dependence or function form of the densities of states and the tunneling amplitudes in the spectral density depends on the detailed QPC electronic structure. Here we perform a model calculation for the QPC-NMR system using a simple Lorentzian spectral density to study the influence of finite bandwidth (cutoff energy) and memory effect on the NMR system dynamics. We will show later in our numerical treatment of the non-Markovian NMR-QPC system that for the parameters we choose, when the bandwidth of the Lorentzian spectral density of Eq. (22) is about $\Lambda_e \leqslant 5\hbar\omega_0$, the time-dependent coefficients, the dynamical variables of the NMR, and the currents through the QPC differ significantly from their Markovian WBL counterparts. This can be understood as follows. As discussed earlier, in the limit of $\Lambda_e \to 0$, only one channel $\epsilon_k^S - \epsilon_q^D = E_i$ is involved in the electron tunneling processes across the QPC barrier. The opposite limit of a very large bandwidth, $\Lambda_e \gg |\epsilon_k^S - \epsilon_q^D - E_i|$, then leads to a channel-mixture regime[33] where great portions of all possible $\epsilon_k^S \rightleftharpoons \epsilon_q^D$ transitions of electron tunneling between the source (left reservoir or lead) and the drain (right reservoir or lead) are allowed, with weight determined by $J_{A,B}(\epsilon_k^S,\epsilon_q^D)$ and with randomness coming from electron scattering determined by the band structure associated with the geometry of the metallic gates in the QPC. The electron-tunneling processes with a more random channel mixture will reduce the QPC reservoir correlation time[33] and therefore suppress the QPC reservoir memory effect on the NMR dynamics. Thus the non-Markovian processes will become significant if the QPC electronic structure can be designed or engineered to have a spectral density with a narrow bandwidth comparable to the (renormalized) resonant frequency of the NMR, as the QPC reservoir correlation time in this case is comparable to the NMR system response time (see also the discussions regarding Figs. 2 and 3 in Sec. VII). The typical frequency of NMR is in the range of a few hundred kilohertz to a few gigahertz. Thus the condition of being able to observe a significant non-Markovian finite-bandwidth behavior of $\Lambda_e \leqslant 5\hbar\omega_0$ suggests that the bandwidth of the QPC spectral density should be in the range of about 1–20 μeV.

With the specified spectral density Eq. (22) and the help of Eqs. (20) and (21), one can rewrite the n-resolved master equation (19) in the form

$$\dot{\rho}_R^{(n)}(t) = -\frac{i}{\hbar}[H_S,\rho_R^{(n)}(t)] + \frac{g_L^0 g_R^0}{\hbar}\left\{\sum_{i=1}^{3} f_F^+(t,eV+\hbar\omega_i)\left[P\rho_R^{(n-1)}(t)P_i^\dagger - \rho_R^{(n)}(t)P_i^\dagger P\right] - \sum_{i=1}^{3} f_B^+(t,-eV-\hbar\omega_i) \times \left[P P_i^\dagger \rho_R^{(n)}(t) - P_i^\dagger \rho_R^{(n+1)}(t)P\right] + \text{H.c.}\right\} + \mathcal{L}_{\text{damp}}\left[\rho_R^{(n)}(t)\right]. \tag{23}$$

Here P_i is defined in Eqs. (15)–(17), $P = \sum_{i=1}^{3} P_i = P_1 + P_2 + P_3$, the values of the frequency ω_i are given by $\omega_1 = 0$, $\omega_2 = -\omega_3 = \omega_0$, and H.c. denotes the Hermitian conjugate of all the previous terms in the curly brackets of Eq. (23). By the change to the new variables $\omega_k^S = \epsilon_k^S - \mu_S$ and $\omega_q^D = \epsilon_q^D - \mu_D$, the time-dependent coefficients $f_{F(B)}^{\pm}$ in Eq. (23) can be written in the following forms:

$$f_F^+(t,eV) = [f_F^-(t,eV)]^\dagger = \frac{1}{\hbar}\int_0^t d\tau \int_{-\infty}^{\infty}\int_{-\infty}^{\infty} d\omega_k^S d\omega_q^D \frac{\Lambda_e^2}{(\omega_k^S - \omega_q^D + eV - E_i)^2 + \Lambda_e^2}\frac{1}{e^{\beta\omega_k^S}+1}\left(1 - \frac{1}{e^{\beta\omega_q^D}+1}\right) \times e^{+i(\omega_k^S - \omega_q^D + eV)\tau/\hbar}, \tag{24}$$

$$f_B^+(t,-eV)=[f_B^-(t,-eV)]^\dagger=\frac{1}{\hbar}\int_0^t d\tau\int_{-\infty}^{\infty}\int_{-\infty}^{\infty}d\omega_k^S d\omega_q^D\frac{\Lambda_e^2}{\left(\omega_k^S-\omega_q^D+eV-E_i\right)^2+\Lambda_e^2}\left(1-\frac{1}{e^{\beta\omega_k^S}+1}\right)\frac{1}{e^{\beta\omega_q^D}+1}\times e^{+i(\omega_k^S-\omega_q^D+eV)\tau/\hbar}, \tag{25}$$

$$f_F^+(t,eV\pm\hbar\omega_0)=[f_F^-(t,eV\pm\hbar\omega_0)]^\dagger=\frac{1}{\hbar}\int_0^t d\tau\int_{-\infty}^{\infty}\int_{-\infty}^{\infty}d\omega_k^S d\omega_q^D\frac{\Lambda_e^2}{\left(\omega_k^S-\omega_q^D+eV-E_i\right)^2+\Lambda_e^2}\frac{1}{e^{\beta\omega_k^S}+1}\left(1-\frac{1}{e^{\beta\omega_q^D}+1}\right)\times e^{+i(\omega_k^S-\omega_q^D+eV\pm\hbar\omega_0)\tau/\hbar}, \tag{26}$$

and

$$f_B^+(t,-eV\mp\hbar\omega_0)=[f_B^-(t,-eV\mp\hbar\omega_0)]^\dagger=\frac{1}{\hbar}\int_0^t d\tau\int_{-\infty}^{\infty}\int_{-\infty}^{\infty}d\omega_k^S d\omega_q^D\frac{\Lambda_e^2}{\left(\omega_k^S-\omega_q^D+eV-E_i\right)^2+\Lambda_e^2}\times\frac{1}{e^{\beta\omega_q^D}+1}\left(1-\frac{1}{e^{\beta\omega_k^S}+1}\right)e^{+i(\omega_k^S-\omega_q^D+eV\pm\hbar\omega_0)\tau/\hbar}. \tag{27}$$

Physically, $f_F^\pm(t,eV)$ and $f_B^\pm(t,-eV)$ describe the memory effects on the NMR system induced by the elastic electron tunneling processes in the QPC reservoirs with no excitation of the NMR. The time-dependent coefficients $f_F^\pm(t,eV\pm\hbar\omega_0)$ and $f_B^\pm(t,-eV\mp\hbar\omega_0)$ describe the memory effects on the NMR system caused by the inelastic electron tunneling processes that involve the NMR excitation and relaxation, respectively.

The effect of the thermal bosonic environment on the master equation in the last line of Eq. (23) can be derived also up to second order in the system-environment coupling strength[48–50] and the result is given as

$$\begin{aligned}\mathcal{L}_{\rm damp}[\rho_R^{(n)}(t)]&=-\frac{i}{\hbar}\left[\frac{M}{2}\tilde{\Omega}_0^2(t)x^2,\rho_R^{(n)}(t)\right]-\frac{i}{\hbar}\gamma_0(t)\left[x,\left\{p,\rho_R^{(n)}(t)\right\}\right]\\&\quad-\frac{1}{\hbar^2}D_0(t)\left[x,\left[x,\rho_R^{(n)}(t)\right]\right]+\frac{1}{\hbar^2}h_0(t)\left[x,\left[p,\rho_R^{(n)}(t)\right]\right],\end{aligned} \tag{28}$$

where the time-dependent coefficients are

$$\tilde{\Omega}_0^2(t)=-\frac{2}{m}\int_0^t d\tau\cos(\omega_0\tau)\eta(\tau), \tag{29}$$

$$\gamma_0(t)=\frac{1}{m\omega_0}\int_0^t d\tau\sin(\omega_0\tau)\eta(\tau), \tag{30}$$

$$D_0(t)=\hbar\int_0^t d\tau\cos(\omega_0\tau)\nu(\tau), \tag{31}$$

$$h_0(t)=-\frac{\hbar}{m\omega_0}\int_0^t d\tau\sin(\omega_0\tau)\nu(\tau). \tag{32}$$

Here $\tilde{\Omega}_0^2(t)$ is the frequency shift due to the coupling to the thermal environment, $\gamma_0(t)$ is the dissipative coefficient, and $D_0(t)$ and $h_0(t)$ represent the diffusion coefficients. The two kernels $\eta(\tau)$ and $\nu(\tau)$ appearing in Eqs. (29)–(32) are so-called dissipation and noise kernels, respectively, and are defined as

$$\eta(\tau)=\int_0^\infty d\omega J(\omega)\sin(\omega\tau) \tag{33}$$

and

$$\nu(\tau)=\int_0^\infty d\omega J(\omega)\cos(\omega\tau)\coth(\beta\hbar\omega/2), \tag{34}$$

where $J(\omega)$ is the spectral density of the bosonic environment defined as

$$J(\omega)=\sum_n\frac{\lambda_n^2}{2m_n\omega_n}\delta(\omega-\omega_n). \tag{35}$$

Again, we could, in principle, deal with any given form of the spectral density. But as a particular example, we use the following form of spectral density with a Lorentz-Drude cutoff function to specify the environment:[48–50,58]

$$J(\omega)=\frac{2}{\pi}m\gamma\omega\left(\frac{\omega}{\Lambda}\right)^{n-1}\frac{\Lambda_0^2}{\Lambda_0^2+\omega^2}, \tag{36}$$

where Λ_0 is the cutoff frequency, γ is a constant characterizing the strength of the interaction with the environment, and m is the mass of the NMR. For simplicity, we will take the commonly used spectral density of an Ohmic bath, i.e., the $n=1$ case in Eq. (36).

The n-resolved master equation (23) with Eq. (28) was derived without making the Markovian and the pretrace and post-trace rotating-wave approximations, and the only approximations we use are the second-order perturbation theory, the initially factorized system-bath density matrix, and the forms of the spectral densities of Eqs. (22) and (36). So the n-resolved master equation is valid for arbitrary bias voltages and environment of temperature, as long as the perturbation theory that we use up to second order in the system-QPC and system-environment coupling strength holds.

IV. UNCONDITIONAL MASTER EQUATION AND MARKOVIAN LIMIT

A. Unconditional master equation

In this section, we present the unconditional master equation for the reduced density matrix of the NMR system. Statistically, the unconditional master equation can be straightforwardly obtained by summing up Eq. (23) over all possible

electron numbers n, i.e., $\rho_R(t) = \sum_n \rho_R^{(n)}$. Despite the different natures of the nonequilibrium fermionic QPC reservoir and the thermal bosonic environment, by combining the relevant terms together, the unconditional non-Markovian master equation can be cast into a simple form similar to the non-Markovian quantum Brownian motion master equation as[76]

$$\begin{aligned}\dot{\rho}_R(t) = &-\frac{i}{\hbar}\left[H_{\rm sys} + \frac{m}{2}\left(\tilde{\omega}_e^2(t) + \tilde{\Omega}_0^2(t)\right)x^2, \rho_R(t)\right] \\ &- \frac{i}{\hbar}[\gamma_e(t) + \gamma_0(t)][x,\{p,\rho_R(t)\}] \\ &- \frac{1}{\hbar^2}[D_e(t) + D_0(t)][x,[x,\rho_R(t)]] \\ &+ \frac{1}{\hbar^2}[h_e(t) + h_0(t)][x,[p,\rho_R(t)]]. \end{aligned} \tag{37}$$

The whole non-Markovian character of the dynamics of the NMR system is contained in the time-dependent coefficients appearing in the master equation. The time-dependent coefficients that come from the QPC electron reservoirs are denoted with a subscript e. The frequency renormalization $\tilde{\omega}_e^2(t)$, the damping coefficient $\gamma_e(t)$, the decoherence coefficient $D_e(t)$, and the diffusion coefficient $h_e(t)$ are, respectively, given by

$$\tilde{\omega}_e^2(t) = \frac{\hbar G_{xx}}{\pi m}\mathrm{Im}\left[\xi_1^a(t) + \xi_2^a(t)\right], \tag{38}$$

$$\gamma_e(t) = \frac{\hbar G_{xx}}{2\pi m\omega_0}\mathrm{Re}\left[\xi_1^a(t) - \xi_2^a(t)\right], \tag{39}$$

$$D_e(t) = \frac{\hbar^2 G_{xx}}{2\pi}\mathrm{Re}\left[\xi_1^s(t) + \xi_2^s(t)\right], \tag{40}$$

$$h_e(t) = \frac{\hbar^2 G_{xx}}{2\pi m\omega_0}\mathrm{Im}\left[\xi_1^s(t) - \xi_2^s(t)\right], \tag{41}$$

where

$$G_{xx} = \frac{2\pi}{\hbar} g_L^0 g_R^0 |\chi_{00}|^2, \tag{42}$$

$$\xi_1^s(t) = f_F^+(t, eV + \hbar\omega_0) + f_B^+(t, -eV - \hbar\omega_0), \tag{43}$$

$$\xi_1^a(t) = f_F^+(t, eV + \hbar\omega_0) - f_B^+(t, -eV - \hbar\omega_0), \tag{44}$$

$$\xi_2^s(t) = f_F^+(t, eV - \hbar\omega_0) + f_B^+(t, -eV + \hbar\omega_0), \tag{45}$$

$$\xi_2^a(t) = f_F^+(t, eV - \hbar\omega_0) - f_B^+(t, -eV + \hbar\omega_0). \tag{46}$$

We note that due to the interaction with the thermal environment, the frequency shift term $\tilde{\Omega}_0^2(t)$ in Eq. (37) diverges as the cutoff frequency $\Lambda_0 \to \infty$ and thus is not physical.[48–50,58] Therefore, a regularization procedure[77,78] is needed for the frequency renormalization. We adopt the view of the renormalization[77,78] to regard the frequency in the original Hamiltonian as a finite renormalized frequency ω_0 and add a frequency counterterm with a frequency[48–50,58] defined as

$$\Omega_c^2 = \frac{1}{m}\sum_n \frac{\lambda_n^2}{m_n\omega_n^2} = \frac{2}{m}\int_0^\infty d\omega \frac{J(\omega)}{\omega} \tag{47}$$

to cancel at large times the frequency shift $\tilde{\Omega}_0^2(t)$. Similar to this reasoning, another frequency counterterm with a frequency ω_c^2 is introduced[21] to compensate at long times the frequency shift $\tilde{\omega}_e^2(t)$ induced as a result of the coupling to the QPC leads (reservoirs). The physical frequency in this case is then $\omega_p^2(t) = \omega_0^2 + \tilde{\omega}_e^2(t) + \tilde{\Omega}_0^2(t) + \omega_c^2 + \Omega_c^2$ and approaches the finite renormalized frequency ω_0 at large times. The non-Markovian master equations (23) and (37) are the main results of this paper.

B. Markovian limit

Next, we show that by taking appropriate limits, our non-Markovian master equations can recover the various Markovian master equations reported in the literature. The Markovian approximation is valid when the bath correlation time is much smaller than the characteristic time scale of the system of interest. The bath correlation time is determined by the bath correlation kernels (functions) and depends on the form of the bath spectral density. We will perform the numerical calculation of the QPC reservoir correlation time in the next section to investigate how the reservoir correlation time is varied as a function of various parameters in the problem.

Here, if we nevertheless take the Markovian approximation of very short bath correlation times of the QPC reservoirs and of the thermal bosonic environment, this is equivalent to assuming that the bath correlation functions (kernels) are δ correlated in time and thus the upper limit t of the time τ integrals in Eqs. (24)–(27) for QPC reservoirs and in Eqs. (29)–(32) for the thermal bosonic bath can be taken to $t \to \infty$. Another commonly used assumption in the Markovian limit is the so-called WBL approximation. This assumption may not seem essential to evaluate the integrations if one already makes the very short bath correlation time approximation. But the assumption of very short bath correlation times can be justified in various models of the bath spectral densities with very large cutoff energies. This has been demonstrated for the bosonic Ohmic bath.[48–50,58] We will show in Sec. VII that this is also the case for the simple Lorentzian spectral density of Eq. (22) for the nonequilibrium QPC fermionic reservoirs. Thus, if we take the Markovian approximation of very short correlation times (integration limit $t \to \infty$), then the time-dependent coefficients in the master equations (23), (28), and (37) become time independent. Specifically, using the relation

$$\lim_{t\to\infty}\int_0^t d\tau e^{i(\omega-\omega_0)\tau} = \pi\delta(\omega-\omega_0) + i\mathrm{P}\left(\frac{1}{\omega-\omega_0}\right), \tag{48}$$

where P indicates the Cauchy principal value, the coefficients $f_{F(B)}^{\pm}$ in Eqs. (24)–(27) coming from the QPC reservoirs can be written as

$$\lim_{t\to\infty} f_{F(B)}^{\pm}(t,y) \equiv W_{F(B)}[y] \pm i\Theta_{F(B)}[y], \tag{49}$$

where

$$W_F[y] = \pi\frac{y}{1-e^{-y/k_BT}}\frac{\Lambda_e^2}{(eV-y+E_i)^2+\Lambda_e^2}, \tag{50}$$

$$W_B[y] = \pi\frac{y}{1-e^{-y/k_BT}}\frac{\Lambda_e^2}{(eV+y+E_i)^2+\Lambda_e^2}, \tag{51}$$

$$\begin{aligned}\Theta_F[y] = &\int_{-\infty}^{\infty}\int_{-\infty}^{\infty} d\omega_k^S d\omega_q^D \frac{\Lambda_e^2}{\left(\omega_k^S-\omega_k^D-E_i\right)^2+\Lambda_e^2}\frac{1}{e^{\beta\omega_k^S}+1} \\ &\times\left(1-\frac{1}{e^{\beta\omega_q^D}+1}\right)\mathrm{P}\left(\frac{1}{\omega_k^S-\omega_q^D+eV+y}\right),\end{aligned} \tag{52}$$

$$\Theta_B[y]=\int_{-\infty}^{\infty}\int_{-\infty}^{\infty}d\omega_k^S d\omega_q^D\frac{\Lambda_e^2}{\left(\omega_k^S-\omega_k^D-E_i\right)^2+\Lambda_e^2}\frac{1}{e^{\beta\omega_q^D}+1}\times\left(1-\frac{1}{e^{\beta\omega_k^S}+1}\right)\mathrm{P}\left(\frac{1}{\omega_k^S-\omega_q^D+eV-y}\right). \tag{53}$$

We note here that we separate the Markovian approximation from the WBL approximation although the Markovian approximation can often be justified by considering a very large cutoff energy. So the cutoff energy Λ_e remains in Eqs. (50)–(53). If the WBL ($\Lambda_e\to\infty$) is taken, then the real parts of $f^{\pm}_{F(B)}(t\to\infty,y)$ when multiplied by the factor $2g_L^0g_R^0A_{00}B_{00}/\hbar$ become the finite-temperature forward (backward) Markovian WBL electron tunneling rates of $\Gamma_{AB}^{MT}(y)=(2\pi/\hbar)g_L^0g_R^0A_{00}B_{00}/[1-\exp(-y/k_BT)]$ in the literature,[19–21,25,28–32] where the value of A_{00} and B_{00} could be either one of the tunneling amplitudes T_{00} and $\tilde{\chi}_{00}$. As a result, in the Markovian limit, the frequency renormalization, the damping coefficient, the decoherence coefficient, and the diffusion coefficient in Eqs. (38)–(41) due to the QPC reservoirs in the WBL ($\Lambda_e\to\infty$) become, respectively,

$$\left(\tilde{\omega}_e^M\right)^2=\frac{\hbar G_{xx}}{\pi m}\{\Theta_F[eV+\hbar\omega_0]-\Theta_B[-eV-\hbar\omega_0]+\Theta_F[eV-\hbar\omega_0]-\Theta_B[-eV+\hbar\omega_0]\}, \tag{54}$$

$$\gamma_e^M=\frac{\hbar^2}{m}G_{xx}, \tag{55}$$

$$D_e^M=\frac{\hbar^2G_{xx}}{2}\left[(eV+\hbar\omega_0)\coth\frac{eV+\hbar\omega_0}{2k_BT}+(eV-\hbar\omega_0)\coth\frac{eV-\hbar\omega_0}{2k_BT}\right], \tag{56}$$

$$h_e^M=\frac{\hbar G_{xx}}{2\pi m\omega_0}\{\Theta_F[eV+\hbar\omega_0]+\Theta_B[-eV-\hbar\omega_0]-\Theta_F[eV-\hbar\omega_0]-\Theta_B[-eV+\hbar\omega_0]\}. \tag{57}$$

Similarly, the frequency renormalization, the damping coefficient, and the diffusion coefficients in Eqs. (29)–(32) due to the Ohmic thermal environment in the Markovian WBL ($\Lambda_0\to\infty$) can also be obtained as[48]

$$\left(\tilde{\Omega}_0^M\right)^2=-\frac{1}{m}\sum_n\frac{\lambda_n^2}{m_n\omega_n^2}=-\frac{2}{m}\int_0^\infty d\omega\frac{J(\omega)}{\omega}=-\Omega_c^2, \tag{58}$$

$$\gamma_0^M=\gamma, \tag{59}$$

$$D_0^M=m\gamma\hbar\omega_0\coth\left(\frac{\hbar\omega_0}{2k_BT}\right), \tag{60}$$

$$h_0^M=\gamma k_BT\sum_{n=-\infty}^{\infty}\frac{-\nu_n}{\left(\nu_n^2+\omega_0^2\right)}, \tag{61}$$

where $\upsilon_n=2\pi nk_BT/\hbar$ are known as the Matsubara frequencies.

We note that our unconditional non-Markovian master equation (37) in the Markovian WBL recovers the Markovian master equation (2.12) in Ref. 21. In the special case of the zero-temperature and high-bias limit where $D_e^M=m\gamma_e^MeV$, we recover Eq. (6) of Ref. 19 if the coefficients coming from the contributions of the thermal bosonic bath are neglected. Similarly, the conditional non-Markovian n-resolved master equation (23) also reduces to the Markovian n-resolved master equation (2.9) in Ref. 21. Taking the high-temperature limit of the bosonic environment and Fourier-transforming in the n index, the conditional n-resolved master equation (23) in the Markovian limit also reduces to Eq. (2) of Ref. 20 if the dc bias case is considered and the transmission phase η is set to zero in Ref. 20. Again, considering only the QPC reservoirs and in the special case of the zero-temperature and high-bias limits, one obtains Eq. (5) of Ref. 19 in the Markovian limit from the conditional n-resolved master equation (23).

V. DYNAMICS OF THE NMR

Using the master equation (37), we can obtain the equation of motion for the mean or expectation value of any physical operation O of the NMR by calculating $\frac{d\langle O\rangle}{dt}=\mathrm{Tr}[O\dot{\rho}_R(t)]$. So the equations of motion of the mean (expectation value) of the position and the momentum are

$$\frac{d\langle x(t)\rangle}{dt}=\frac{\langle p(t)\rangle}{m}, \tag{62}$$

$$\frac{d\langle p(t)\rangle}{dt}=-m\omega_p^2(t)\langle x(t)\rangle-2[\gamma_e(t)+\gamma_0(t)]\langle p(t)\rangle, \tag{63}$$

and for the second moments we obtain

$$\frac{d\langle x^2(t)\rangle}{dt}=\frac{1}{m}\langle\{x,p\}(t)\rangle, \tag{64}$$

$$\frac{d\langle p^2(t)\rangle}{dt}=-m\,\omega_p^2(t)\langle\{x,p\}(t)\rangle-4[\gamma_e(t)+\gamma_0(t)]\langle p^2(t)\rangle+2[D_e(t)+D_0(t)], \tag{65}$$

$$\frac{d\langle\{x,p\}(t)\rangle}{dt}=2\frac{\langle p^2(t)\rangle}{m}-2m\omega_p^2(t)\langle x^2(t)\rangle-2[\gamma_e(t)+\gamma_0(t)]\times\langle\{x,p\}(t)\rangle+2[h_e(t)+h_0(t)]. \tag{66}$$

Combining Eqs. (62) and (63) yields

$$\frac{d^2\langle x(t)\rangle}{dt^2}+2\gamma_{\mathrm{tot}}(t)\frac{d\langle x(t)\rangle}{dt}+\omega_p^2(t)\langle x(t)\rangle=0, \tag{67}$$

where $\gamma_{\mathrm{tot}}=\gamma_e+\gamma_0$.

One may in principle solve the time evolutions of the differential equations (62)–(66) and the numerical results will be presented in Sec. VII. Simple analytical expressions of the steady-state ($t\to\infty$) solutions can, however, be obtained as[79]

$$\langle x\rangle_{t\to\infty}=\langle p\rangle_{t\to\infty}=0, \tag{68}$$

$$\langle\{x,p\}\rangle_{t\to\infty}=0, \tag{69}$$

$$\langle x^2\rangle_{t\to\infty}=\lim_{t\to\infty}\frac{1}{2m\omega_p^2(t)}\left(\frac{D_e(t)+D_0(t)}{m[\gamma_e(t)+\gamma_0(t)]}+2[h_e(t)+h_0(t)]\right), \tag{70}$$

$$\langle p^2\rangle_{t\to\infty}=\lim_{t\to\infty}\frac{D_e(t)+D_0(t)}{2[\gamma_e(t)+\gamma_0(t)]}. \tag{71}$$

For the moment, let us consider the case where the influence of the thermal environment is neglected. We also note that, for typical values of finite electric reservoir temperatures and finite electric bias voltages, the diffusion coefficient $h_e(t)/\hbar$ is generally much smaller than $D_e(t)/p_0^2$ and $\gamma_e(t)$ and thus is often neglected. In this case, we obtain from Eqs. (70), (55), and (56) the steady-state $\langle x^2\rangle_{t\to\infty}$ in the WBL as

$$\langle x^2\rangle_{t\to\infty}=\frac{\left[(eV+\hbar\omega_0)\coth\frac{eV+\hbar\omega_0}{2k_BT}+(eV-\hbar\omega_0)\coth\frac{eV-\hbar\omega_0}{2k_BT}\right]}{4m\omega_0^2}. \tag{72}$$

At zero temperature ($k_BT=0$) and low voltages ($eV\ll\hbar\omega_0$), we have $\langle x^2\rangle\approx\frac{\hbar}{2m\omega_0}$. In this case, the NMR is in the ground state and is independent of the bias voltage as the bias voltage is unable to excite the NMR from its ground state. On the other hand, at high voltages ($eV\gg\hbar\omega_0$), the NMR is no longer in the ground state and $\langle x^2\rangle\approx\frac{eV}{2m\omega_0^2}$.[21] At high temperatures ($k_BT\gg eV,\ \hbar\omega_0$), the quantum mean square of the position of the NMR becomes $\langle x^2\rangle\approx\frac{k_BT}{m\omega_0^2}$ which is expected from a classical oscillator in thermal equilibrium.

VI. TRANSPORT CURRENT

With the n-resolved time-convolutionless master equation for $\rho_R^{(n)}(t)$, one is readily able to compute the transport current $I(t)=e\frac{d\langle N(t)\rangle}{dt}$, where $\langle N(t)\rangle=\sum_n nP(n,t)=\sum_n n\mathrm{Tr}[\rho_R^{(n)}(t)]$ is the expectation value of the number of electrons that have tunneled into the right lead (drain) in time t. Here Tr means tracing the density matrix over the degrees of freedom of the NMR system. Inserting Eq. (23) into $I(t)=e\sum_n n\mathrm{Tr}[\dot\rho_R^{(n)}(t)]$ gives rise to[20,21,24–27,29,31,32]

$$\frac{I(t)}{e}=\frac{g_L^0g_R^0}{\hbar}\sum_{i=1}^{3}\mathrm{Tr}\{[f_F^+(t,eV+\hbar\omega_i)P_i^\dagger P\rho_R(t)-f_B^+(t,-eV-\hbar\omega_i)PP_i^\dagger\rho_R(t)]+\mathrm{H.c.}\}. \tag{73}$$

Here $\rho_R(t)=\sum_n\rho_R^{(n)}(t)$ is the unconditional density matrix of the NMR. This non-Markovian average current is valid for arbitrary QPC lead temperatures and arbitrary bias voltages as long as the second-order perturbation theory holds. We follow Ref. 21 to categorize the non-Markovian average current, Eq. (73), into four physically distinct contributions. Using the definition of $P=\sum_{i=1}^3P_i$ and the definition of P_i in Eqs. (15)–(17), we write the non-Markovian average current Eq. (73) as

$$\frac{I(t)}{e}=\frac{I_{\mathrm{position}}(t)}{e}+\frac{I_P(t)}{e}+\frac{I_{QM}(t)}{e}+\frac{I_{\{X,P\}}(t)}{e}. \tag{74}$$

The first term in Eq. (74) depends on the oscillation position of the NMR and can be written as

$$\frac{I_{\mathrm{position}}(t)}{e}=\frac{1}{2\pi}\Delta_1(t)[G_0+G_x\langle x(t)\rangle]+\frac{1}{4\pi}[\Delta_2(t)+\Delta_3(t)]\times[G_x\langle x(t)\rangle+G_{xx}\langle x^2(t)\rangle]. \tag{75}$$

It reduces in the Markovian WBL to the so-called Ohmic-like part of the current proportional to the conductance defined in Ref. 21. In Eq. (75), the term with conductance $G_0=\frac{2\pi}{\hbar}g_L^0g_R^0|T_{00}|^2$ represents the current through the isolated QPC junction, and the remaining terms due to the coupling to the NMR with conductances $G_x=\frac{2\pi}{\hbar}g_L^0g_R^0\mathrm{Re}[T_{00}^\dagger\chi_{00}]$ and $G_{xx}=\frac{2\pi}{\hbar}g_L^0g_R^0|\chi_{00}|^2$ contribute to the nonlinear part of the current-voltage characteristics[21,80] as the state of the NMR will depend on the bias voltage. The time-dependent coefficients $\Delta_i(t)$ in the non-Markovian region can be written as

$$\Delta_1(t)=f_F^+(t,eV)-f_B^+(t,-eV)+f_F^-(t,eV)-f_B^-(t,-eV)=2\mathrm{Re}[f_F^+(t,eV)-f_B^+(t,-eV)], \tag{76}$$

$$\Delta_2(t)=f_F^+(t,eV+\hbar\omega_0)-f_B^+(t,-eV-\hbar\omega_0)+f_F^-(t,eV+\hbar\omega_0)-f_B^-(t,-eV-\hbar\omega_0)=2\mathrm{Re}\big[\xi_1^a(t)\big], \tag{77}$$

$$\Delta_3(t)=f_F^+(t,eV-\hbar\omega_0)-f_B^+(t,-eV+\hbar\omega_0)+f_F^-(t,eV-\hbar\omega_0)-f_B^-(t,-eV+\hbar\omega_0)=2\mathrm{Re}\big[\xi_2^a(t)\big], \tag{78}$$

where $\xi_1^a(t)$ and $\xi_2^a(t)$ are defined in Eqs. (44) and (46), respectively. The second term in Eq. (74), $I_P(t)/e$, is proportional to the average velocity of the oscillator,

$$\frac{I_P(t)}{e}=\frac{G_p}{4\omega_0\pi m}[\Delta_2(t)-\Delta_3(t)]\langle p(t)\rangle. \tag{79}$$

This term is nonvanishing only for an asymmetric junction,[21] $G_p=\frac{2\pi}{\hbar}g_L^0g_R^0\mathrm{Im}[T_{00}^\dagger\chi_{00}]\neq0$. The third term in Eq. (74), $I_{QM}(t)$, derived from the commutator of position and momentum operators, is referred to as the quantum correction to the current,[21]

$$\frac{I_{QM}(t)}{e}=-\frac{\hbar G_{xx}}{8\pi m\omega_0}[\Delta_4(t)-\Delta_5(t)]. \tag{80}$$

Here the time-dependent coefficients $\Delta_4(t)$ and $\Delta_5(t)$ can be written as

$$\Delta_4(t)=f_F^+(t,eV+\hbar\omega_0)+f_B^+(t,-eV-\hbar\omega_0)+f_F^-(t,eV+\hbar\omega_0)+f_B^-(t,-eV-\hbar\omega_0)=2\mathrm{Re}\big[\xi_1^s(t)\big], \tag{81}$$

$$\Delta_5(t)=f_F^+(t,eV-\hbar\omega_0)+f_B^+(t,-eV+\hbar\omega_0)+f_F^-(t,eV-\hbar\omega_0)+f_B^-(t,-eV+\hbar\omega_0)=2\mathrm{Re}\big[\xi_2^s(t)\big], \tag{82}$$

where $\xi_1^s(t)$ and $\xi_2^s(t)$ are defined in Eqs. (43) and (45), respectively. By using Eqs. (49)–(51) in the Markovian WBL (i.e., taking $\Lambda_e\to\infty$), the above three terms that contribute to the total current recover their respective Markovian versions presented in Ref. 21:

$$\frac{I^M_{\mathrm{position}}}{e}=eV[G_0+2G_x\langle x(t)+G_{xx}\langle x^2(t)\rangle], \tag{83}$$

$$\frac{I_P^M}{e}=\frac{G_p\hbar}{m}\langle p(t)\rangle, \tag{84}$$

$$\frac{I_{QM}^M}{e}=-\frac{\hbar G_{xx}}{4m\omega_0}\left[(eV+\hbar\omega_0)\coth\frac{eV+\hbar\omega_0}{2k_BT}-(eV-\hbar\omega_0)\coth\frac{eV-\hbar\omega_0}{2k_BT}\right]. \tag{85}$$

The last term in Eq. (74), $I_{\{X,P\}}(t)/e$, is an additional term that was not discussed in Ref. 21. This term originates from the symmetrized product of the position and momentum operators and can be written as

$$\frac{I_{\{X,P\}}(t)}{e} = \frac{iG_{xx}}{4m\omega_0\pi}[\Delta_6(t) - \Delta_7(t)]\langle(xp+px)(t)\rangle, \quad (86)$$

where

$$\begin{aligned}\Delta_6(t) &= f_F^+(t,eV+\hbar\omega_0) - f_B^+(t,-eV-\hbar\omega_0) \\ &\quad - f_F^-(t,eV+\hbar\omega_0) + f_B^-(t,-eV-\hbar\omega_0) \\ &= 2i\mathrm{Im}\big[\xi_1^a(t)\big], \end{aligned} \quad (87)$$

$$\begin{aligned}\Delta_7(t) &= f_F^+(t,eV-\hbar\omega_0) - f_B^+(t,-eV+\hbar\omega_0) \\ &\quad - f_F^-(t,eV-\hbar\omega_0) + f_B^-(t,-eV+\hbar\omega_0) \\ &= 2i\mathrm{Im}\big[\xi_2^a(t)\big], \end{aligned} \quad (88)$$

and $\xi_1^a(t)$ and $\xi_2^a(t)$ are defined in Eqs. (44) and (46), respectively. In the Markovian limit, this term becomes

$$\begin{aligned}\frac{I^M_{\{X,P\}}}{e} &= \frac{G_{xx}}{2m\omega_0\pi}[\,\Theta_F(eV+\hbar\omega_0) - \Theta_B(-eV-\hbar\omega_0) \\ &\quad - \Theta_F(eV-\hbar\omega_0) + \Theta_B(-eV+\hbar\omega_0)]\langle(xp+px)(t)\rangle, \end{aligned} \quad (89)$$

where the functions $\Theta_F(x)$ and $\Theta_B(x)$ are defined in Eqs. (52) and (53), respectively. This extra current term Eq. (86), with a coefficient coming from the combination of the imaginary parts of the QPC reservoir correlation functions, was generally ignored in the studies of the same problem in the literature.[19–23] The contribution to the diffusion coefficient $h_e(t)$, Eq. (41), also comes from the imaginary parts of the QPC reservoir correlation functions but with a different combination. Unlike the diffusion coefficient $h_e(t)$, which is generally much smaller than the other decoherence and damping coefficients for typical parameters and is thus often neglected, we will show in the next section that Eq. (86) has a substantial contribution to the total transient current in the non-Markovian case and differs qualitatively and quantitatively from its Markovian WBL counterpart, Eq. (89) with $\Lambda_e \to \infty$. Thus it may serve as a witness or signature of finite-bandwidth non-Markovian features for the coupled NMR-QPC system.

VII. NUMERICAL RESULTS AND ANALYSIS

In our numerical calculations, we first concentrate on the case where the influence of the thermal environment is neglected. This allows us to address the non-Markovian effect coming solely from the QPC reservoirs. This case where the effect of the QPC reservoirs dominates over that of the thermal environment may nevertheless be justified for a much larger relative coupling strength of QPC to the NMR and for typical QPC bias voltages and reservoir temperatures. We will discuss in Sec. VII B the case when the effect of the thermal environment is included and is comparable to that of the QPC reservoirs.

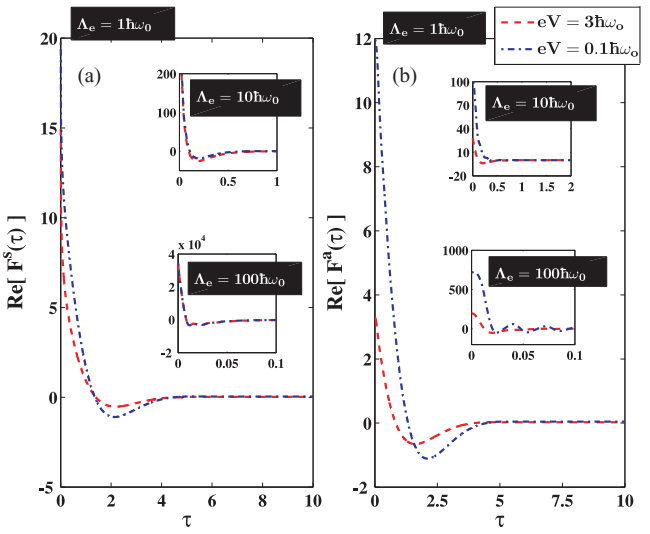

FIG. 2. (Color online) Real part of (a) the symmetric reservoir correlation kernel (function) $F^S(\tau)$ and (b) the antisymmetric reservoir correlation kernel (function) $F^a(\tau)$ at a small Lorentzian cutoff energy of $\Lambda_e = \hbar\omega_0$ for different values of the bias voltage: $(eV/\hbar\omega_0) = 0.1$ (blue dot-dashed lines) and 3 (red dashed lines). The time is in units of ω_0^{-1}. The insets in (a) and (b) are for the cases of $(\Lambda_e/\hbar\omega_0) = 10$ and 100, respectively. The other parameter used is $k_BT = 0.1\hbar\omega_0$.

A. Effect of only the QPC reservoirs

Figures 2(a) and 2(b) show the dependence of real parts of the mode-independent two-time symmetric and antisymmetric QPC reservoir correlation kernels (functions) on the time difference $\tau = t - t_1$ for various values of the cutoff energy Λ_e. The mode-independent two-time symmetric and antisymmetric QPC reservoir correlation kernels (functions) are evaluated by converting the summations over k,k' and q,q' of the mode-dependent correlation functions (kernels) of Eqs. (20) and (21) into energy integrations with the Lorentzian spectral density given by Eq. (22), and then performing the energy integrations. There are several characteristic time scales in this non-Markovian problem. The time scale of the NMR is about $1/\omega_0$, the time scale of the energy-dependent QPC spectral density is about $\hbar/\Lambda_e$, the time scale of the applied bias is $\hbar/eV$, the time scale of the QPC reservoir temperature is $\hbar/k_BT$, the time scale of the electron tunneling is about $1/\Gamma^M_{AB}$, and the time scales of the combinations of the electron tunneling rates are p_0^2/D_e^M, $1/\gamma_e^M$, and $\hbar/h_e^M$. We define the time scale at which the profiles of the QPC reservoir two-time correlation kernels (functions) decay as the QPC bath correlation time τ_B. We can see from Figs. 2(a) and 2(b) that at a given low cutoff energy of $\Lambda_e = \hbar\omega_0$ and at a low temperature of $k_BT = 0.1\hbar\omega_0$, the reservoir two-time correlation kernel (function) with a high bias voltage of $eV = 3\hbar\omega_0$ (in red dashed lines) has a slightly shorter reservoir correlation time τ_B than that with a low bias voltage of $eV = 0.1\hbar\omega_0$ (in blue dot-dashed lines). But as indicated in the insets of Figs. 2(a) and 2(b), the dependence of τ_B on the bias voltage is much weaker than that on the cutoff energy Λ_e. The insets show that the larger is the cutoff energy Λ_e, the smaller is the bath correlation time τ_B. Moreover, the bath correlation time in this case is about $\tau_B \sim \hbar/\Lambda_e$.

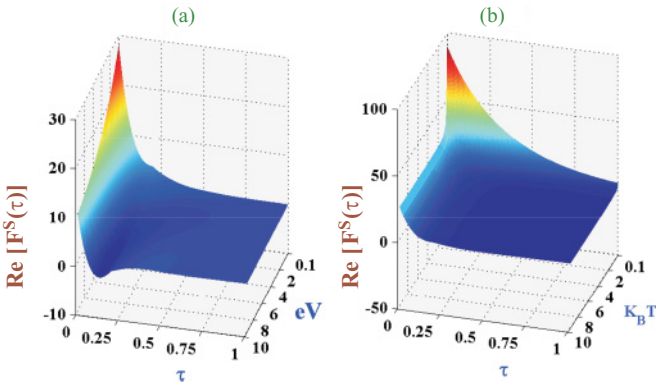

FIG. 3. (Color online) (a) Real part of the symmetric reservoir correlation kernel (function) $F^S(\tau)$ as a function of the time difference $\tau = t - t_1$ and the bias voltage eV. The bias voltage is in units of $\hbar\omega_0$ and the time is in units of ω_0^{-1}. Other parameters used are $\Lambda_e = \hbar\omega_0$ and $k_BT = 0.1\hbar\omega_0$. (b) Real part of the symmetric reservoir correlation kernel (function) $F^S(\tau)$ as a function of the time difference $\tau = t - t_1$ and the QPC lead temperature k_BT. The lead temperature is in units of $\hbar\omega_0$ and the time is in units of ω_0^{-1}. Other parameters used are $\Lambda_e = \hbar\omega_0$ and $eV = 0.1\hbar\omega_0$.

Figure 3(a) shows the symmetric reservoir correlation kernel (function) which depends on bias voltage eV and time difference $\tau = t - t_1$ for a cutoff energy of $\Lambda_e = 1.0\hbar\omega_0$. Although the bath correlation time is affected mainly by the value of the cutoff energy Λ_e, one can still see for the Lorentzian spectral density Eq. (22) chosen here that when the bias voltage decreases, the bath correlation time τ_B increases. Figure 3(b) shows the dependence of the symmetric reservoir correlation kernel (function) on temperature k_BT. Similar to the dependence of the correlation time on the bias voltage, the correlation time increases when the reservoir temperature decreases. The effect of the temperature on the bath correlation time seems to be stronger than that of the bias voltage. The Markovian approximation is valid in the case when the bath correlation time τ_B is much smaller than the typical system response time τ_S. The typical response time of our NMR system is about the minimum value of $(1/\omega_0, 1/\Gamma^M_{AB}, p_0^2/D_e, 1/\gamma_e, \hbar/h_e)$.

Figures 4, 5, and 6 show the real parts of some typical time-dependent coefficients $f^{\pm}_{F(B)}$ of the n-resolved master equation for different values of the bias voltage and temperature, respectively. The cutoff energy Λ_e is also varied in each subplot. Physically, these coefficients, if multiplied by the factor $2g_L^0 g_R^0 A_{00} B_{00}/\hbar$ (where the value of A_{00} and B_{00} could be either one of the tunneling amplitudes T_{00} and $\tilde{\chi}_{00}$), correspond to the time-dependent finite-temperature forward (backward) inelastic QPC electron tunneling rates that accompany with the absorption or emission of the NMR energy quanta. Compared to their Markovian counterparts which are constants in time plotted in dashed lines in Figs. 4, 5, and 6, the memory effects of the QPC reservoirs are contained in the time-dependent coefficients. As the cutoff energy Λ_e is increased, the profiles (peaks) of the time-dependent coefficients become higher and the widths at half maximum become narrower. Moreover, the positions of the peaks of the profiles also shift to the short-time region. In other words, the memory effects of the non-Markovian time-dependent coefficients persist for longer times for smaller values of the cutoff energy. We distinguish the Markovian case, where the cutoff energy Λ_e is finite, from the Markovian WBL case, where the spectral

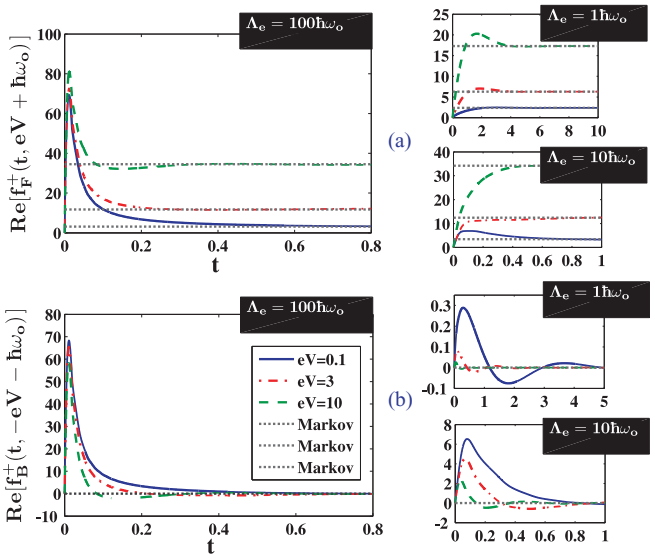

FIG. 4. (Color online) Real parts of the time-dependent forward (backward) inelastic electron tunneling coefficients for different values of the QPC bias voltage: $(eV/\hbar\omega_0) = 0.1$ (in blue solid lines), 3 (in red dot-dashed lines), and 10 (in green dashed lines). The Markovian cases with finite cutoff energies are plotted in gray dotted lines. The time is in units of ω_0^{-1}. Other parameters used are $k_BT = 0.1\hbar\omega_0$ and $\Lambda_e = 100\hbar\omega_0$. The small subplots in (a) and (b) are for the cases of $(\Lambda_e/\hbar\omega_0) = 1$ and 10, respectively. The other parameter used is $k_BT = 0.1\hbar\omega_0$.

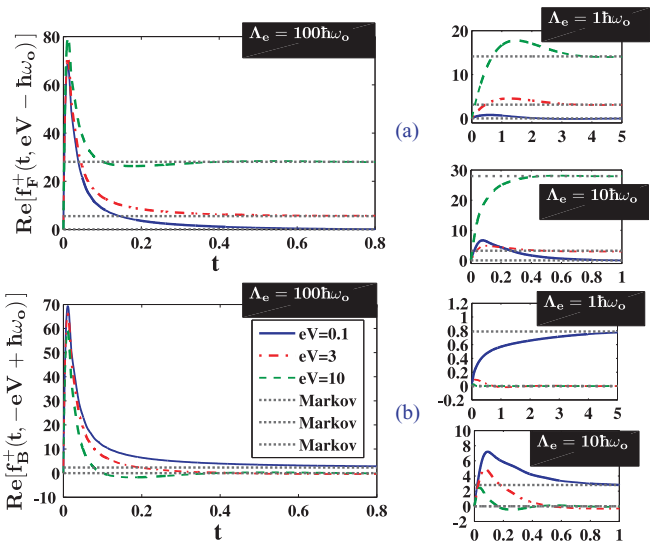

FIG. 5. (Color online) Real parts of the time-dependent forward (backward) inelastic electron tunneling coefficients for different values of the QPC bias voltage: $(eV/\hbar\omega_0) = 0.1$ (in blue solid lines), 3 (in red dot-dashed lines), and 10 (in green dashed lines). The Markovian cases with finite cutoff energy are plotted in gray dotted lines. The time is in units of ω_0^{-1}. Other parameters used are $k_BT = 0.1\hbar\omega_0$ and $\Lambda_e = 100\hbar\omega_0$. The small subplots in (a) and (b) are for the cases of $(\Lambda_e/\hbar\omega_0) = 1$ and 10, respectively. The other parameter used is $k_BT = 0.1\hbar\omega_0$.

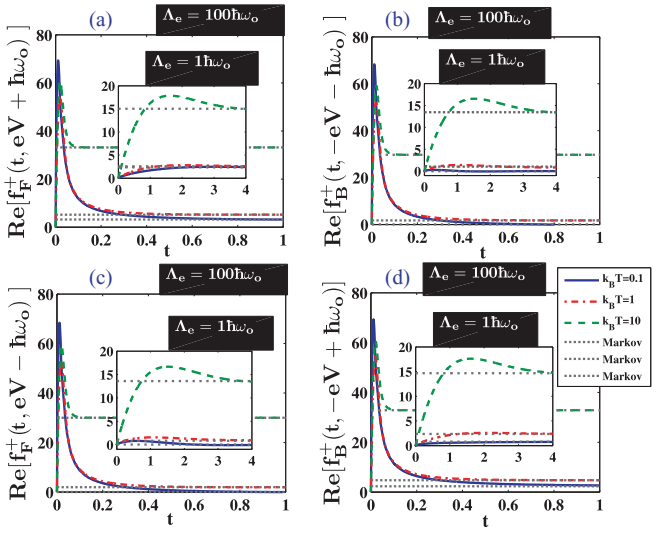

FIG. 6. (Color online) Real parts of the time-dependent forward (backward) inelastic electron tunneling coefficients for different values of the QPC lead temperatures: $(k_BT/\hbar\omega_0) = 0.1$ (in blue solid lines), 1 (in red dot-dashed lines), and 10 (in green dashed lines). The Markovian cases with finite cutoff energy are plotted in gray dotted lines. The time is in units of ω_0^{-1}. Other parameters used are $eV = 0.1\hbar\omega_0$ and $\Lambda_e = 100\hbar\omega_0$. The inset in each subplot is for the case of $eV = 0.1\hbar\omega_0$ and the small Lorentzian cutoff energy of $\Lambda_e = \hbar\omega_0$.

density becomes energy independent as $\Lambda_e \to \infty$. So one can also see that the time-dependent coefficients approach their respective long-time Markovian counterparts of Eqs. (50) and (51) with finite cutoff energies (bandwidths). Furthermore, the non-Markovian coefficients with larger cutoff energies approach more rapidly in time to their Markovian counterparts.

Generally speaking, for the inelastic forward tunneling coefficients in Figs. 4(a), 5(a), 6(a), and 6(b), when the values of the temperature and bias voltage are higher, the long-time asymptotic (Markovian) values of the time-dependent coefficients are larger but the time scales for the time-dependent coefficients approaching their long-time values become shorter. The inelastic (emission) backward tunneling coefficients in Fig. 4(b) approach, at a rather low temperature of $k_BT = 0.1\hbar\omega_0$, approximately zero (the Markovian value) at long times since the argument of $(-eV - \hbar\omega_0)$ is negative [see Eq. (51)]. Similarly, since the argument of $(eV - \hbar\omega_0)$ for a low bias voltage of $eV = 0.1\hbar\omega_0$ is negative, the inelastic (emission) forward tunneling coefficients in blue solid lines in Fig. 5(a) also approach, at a low temperature, approximately zero (the Markovian value) at long times. On the other hand, in Fig. 5(b), since the argument $(-eV + \hbar\omega_0)$ for $eV = 0.1\hbar\omega_0$ is positive, the phonon-assisted backward tunneling is allowed even in the negatively biased direction at a low temperature and thus the inelastic tunneling coefficients in blue solid lines become finite at large times. One can see from Figs. 4 and 5 that if the bias voltage is increased, the inelastic forward tunneling coefficients in Figs. 4(a) and 5(a) are enhanced while the inelastic backward tunneling coefficients in Figs. 4(b) and 5(b) are suppressed. Unlike the cases of $eV = 0.1\hbar\omega$ in Figs. 4(b) and 5(a), the time-dependent inelastic tunneling coefficients (in red dot-dashed lines and in green dashed lines) in Figs. 6(b) and 6(c) approach finite nonzero values for large temperatures even though their arguments of $(-eV - \hbar\omega_0)$ and $(eV - \hbar\omega_0)$ are negative. Moreover, the non-Markovian coefficients with a large cutoff energy of $\Lambda_e = 100\hbar\omega$ shown in Fig. 6 approach their corresponding Markovian counterparts more rapidly as the value of the temperature becomes higher. As in the case of increasing temperature, the time-dependent non-Markovian coefficients with large cutoff energies saturate to their corresponding Markovian counterparts more quickly as the bias voltage is increased as shown in Figs. 4 and 5. In summary, the characteristic times for the non-Markovian behaviors of the time-dependent coefficients $f^{\pm}_{F(B)}$ to differ from their Markovian counterparts are usually longer for smaller cutoff energies, bias voltages, and temperatures.

Next we discuss the time-dependent coefficients of the unconditional master equation defined in Eqs. (38)–(41). We plot in Figs. 7(a), 7(b), 7(c), and 7(d) the time-dependent decoherence coefficient $D_e(t)$, damping coefficient $\gamma_e(t)$, diffusion coefficients $h_e(t)$, and frequency renormalization shift $[\tilde{\omega}_e^2(t) + \omega_c^2]$, respectively, for different values of the Lorentzian cutoff energy Λ_e. The time-dependent coefficients are affected primarily by the values of cutoff energy Λ_e for small fixed values of bias voltage $eV = 0.1\hbar\omega_0$ and temperature $k_BT = 0.1\hbar\omega_0$, and approach their long-time-limit values on a time scale of about $\hbar/\Lambda_e$. The time-dependent coefficients with large cutoff energies saturate at their corresponding Markovian WBL values (in dotted

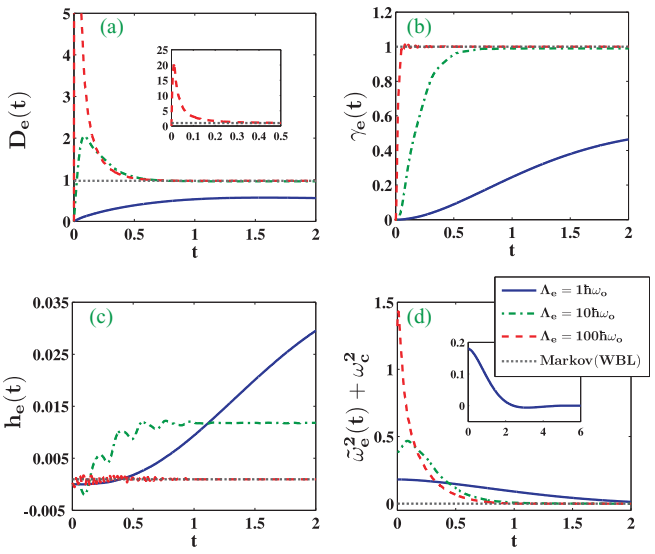

FIG. 7. (Color online) Time-dependent coefficients of the unconditional master equation. (a) Decoherence coefficient $D_e(t)$ in units of $p_0^2\gamma_e^M$, (b) damping coefficient $\gamma_e(t)$ in units of γ_e^M, (c) diffusion coefficients $h_e(t)$ in units of $\hbar\gamma_e^M$, and (d) frequency renormalization shift $[\tilde{\omega}_e^2(t) + \omega_c^2]$ in units of $\omega_0\gamma_e^M$ for different values of the finite Lorentzian cutoff energy: $(\Lambda_e/\hbar\omega_0) = 1$ (in blue solid lines), 10 (in green dashed lines), and 100 (in red dot-dashed lines). The Markovian WBL cases are plotted in gray dotted lines. The time is in units of ω_0^{-1}. The inset in (a) shows the large-value behavior of $D_e(t)$ in the short-time regime for the case of $\Lambda_e = 100\hbar\omega_0$, and the inset in (d) shows the long-time behavior of the frequency renormalization shift $[\tilde{\omega}_e^2(t) + \omega_c^2]$ for the case of $\Lambda_e = \hbar\omega_0$. Other parameters used are $eV = 0.1\hbar\omega_0$ and $k_BT = 0.1\hbar\omega_0$.

lines), while the coefficient with a small cutoff energy of $\Lambda_e = \hbar\omega_0$ approach a long-time value different from the Markovian WBL value. The contribution to the frequency normalization $\tilde{\omega}_e^2(t)$ comes from the imaginary part of the combination of the time-dependent tunneling coefficients [see Eq. (38)] or the combination of the QPC reservoir correlation kernels (functions). We can see from Fig. 7(d) that the frequency renormalization shift $[\tilde{\omega}_e^2(t) + \omega_c^2]$ approaches zero at large times since the counterterm frequency contribution ω_c^2 compensates the frequency renormalization at large times, i.e., $\omega_c^2 = -(\tilde{\omega}_e^M)^2$. The diffusion coefficient $h_e(t)$ coming from the contributions of the imaginary part of the combination of the tunneling coefficients [see Eq. (41)] or the imaginary part of the combination of the reservoir correlation kernels or functions (or coming from the contributions of the Cauchy principal values in the Markovian case) is typically very small compared to the other coefficients (see Fig. 7) and thus is often neglected in the discussion of the reduced dynamics of the NMR. We will show later that a transient current term coming also from the contributions of the imaginary parts of the reservoir kernels with a different combination has, however, a substantial value and should be kept in order to describe correctly the measured time-dependent current.

Figure 8 shows the numerical results of the dimensionless mean and covariance values of the dynamical variables of the NMR for different values of the cutoff energy. The dimensionless mean values $\langle x(t)\rangle/x_0$ and $\langle p(t)\rangle/p_0$ oscillate with a frequency of about the NMR renormalized frequency ω_0 while the variances $\langle x^2(t)\rangle/x_0^2$ and $\langle x(t)p(t) + p(t)x(t)\rangle/x_0p_0$ oscillate with twice the frequency. As expected, the non-Markovian results with larger cutoff energies Λ_e are closer to their Markovian WBL results, and there are considerable differences between the Markovian WBL cases and the non-Markovian cases with the cutoff energies Λ_e comparable to the NMR frequency ω_0. We note here that our results include the frequency renormalization in the non-Markovian cases. We can see from Fig. 7(d) that the non-Markovian cases with larger cutoff energies have a slightly larger renormalized physical frequency in the short-time region. As a result, the initial oscillatory behaviors of $\langle x(t)\rangle/x_0$ and $\langle p(t)\rangle/p_0$ with larger Λ_e in Figs. 8(a) and 8(b) are slightly lower (i.e., with a slightly larger frequency) in the short-time region than that of the Markovian WBL case (in dotted line). Furthermore, one can also observe that the dynamical variables with larger cutoff energies Λ_e approach their steady-state values faster than those with smaller cutoff energies, and the steady-state values of the dynamical variables in Fig. 8 match well the values of the analytical expression of Eqs. (68)–(70) and (72).

Figure 9 shows the differences in the time evolutions of the individual contribution terms of the average current Eq. (74) between the Markovian WBL case and the non-Markovian cases with a small cutoff energy of $\Lambda_e = \hbar\omega_0$. We further divide the first term in Eq. (74), i.e., Eq. (75), into three parts: the isolated QPC tunneling current, the current proportional to $\langle x(t)\rangle$, and the current proportional to $\langle x^2(t)\rangle$. These three parts are plotted in Figs. 9(a), 9(b), and 9(c), respectively. The last three terms of the total current Eq. (74) are plotted in Figs. 9(d),

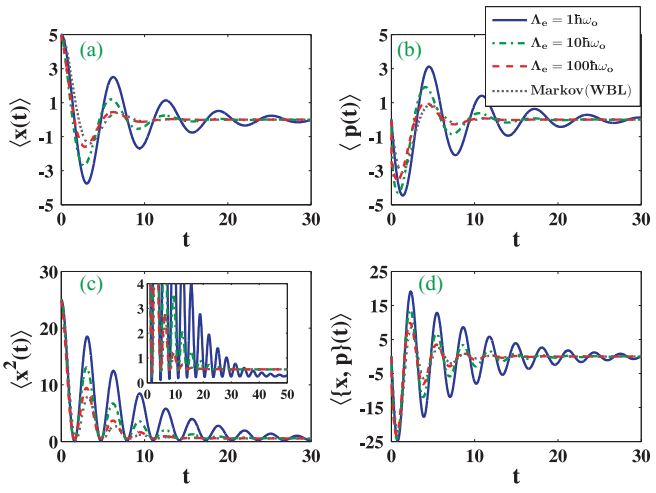

FIG. 8. (Color online) Time evolutions of the dynamical variables of the NMR for different values of the finite Lorentzian cutoff energy: $(\Lambda_e/\hbar\omega_0) = 1$ (in blue solid lines), 10 (in green dot-dashed lines), and 100 (in red dashed lines). (a) Position $\langle x(t)\rangle$ in units of x_0, (b) momentum $\langle p(t)\rangle$ in units of p_0, (c) second-moment position $\langle x^2(t)\rangle$ in units of x_0^2, and (d) symmetrized second-moment position-momentum $\langle\{x, p\}(t)\rangle$ in units of x_0p_0. The Markovian WBL cases are plotted in gray dotted lines. The NMR is initially in a coherent state with $\langle x(0)\rangle = 5x_0$ and $\langle p(0)\rangle = 0$. The time is in units of ω_0^{-1}. The inset in (c) shows the long-time behavior of (c) for small values of $\langle x^2(t)\rangle$. Other parameters used are $eV = 0.1\hbar\omega_0$, $k_BT = 0.1\hbar\omega_0$, and $\gamma_e^M = 0.12\omega_0$.

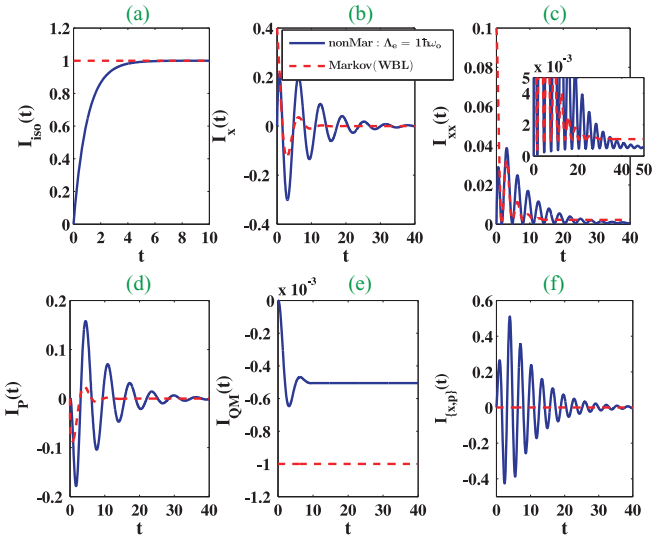

FIG. 9. (Color online) Individual contributions of the average current $I(t)$ of Eq. (74) for the Markovian WBL case (in red dashed lines) and the non-Markovian cases with a small cutoff energy of $\Lambda_e = \hbar\omega_0$ (in blue solid lines). The first term in Eq. (74), i.e., Eq. (75), is divided into three parts: (a) the isolated QPC tunneling current, (b) the current proportional to $\langle x(t)\rangle$, and (c) the current proportional to $\langle x^2(t)\rangle$. The last three terms of the average current Eq. (74) are plotted in (d), (e), and (f), respectively. Each individual contribution of the average current is in units of $I_{iso}^M = e^2VG_0$ and the time is in units of ω_0^{-1}. The inset in (c) shows the long-time behavior of (c) for small values of $I_{XX}(t)$. Other parameters used are $eV = 0.1\hbar\omega_0$, $k_BT = 0.1\hbar\omega_0$, $G_xx_0/G_0 = 0.04$, $G_px_0/G_0 = 0.01$, $G_{xx}x_0^2/G_0 = 0.002$, and $\gamma_e^M = 0.12\omega_0$.

9(e), and 9(f), respectively. There are considerable differences between the non-Markovian and Markovian WBL results. In particular, the tunneling coefficients in the Markovian WBL are constants in time, and thus the coefficients Δ_i in front of the individual contributions to the total average current become also time independent. As a result, the initial values of the individual contribution terms of the average current will depend only on the initial values of the dynamical variables of the NMR. For example, we choose an initial state such that $\langle x(0)\rangle \neq 0$ and $\langle x^2(0)\rangle \neq 0$. Then the Markovian WBL current contributions $I_X(t)$ and $I_{XX}(t)$ start at a finite value at time $t = 0$, i.e., the QPC responds instantaneously to the motion of the NMR to generate a finite current at $t = 0$ (see the red dashed lines in Fig. 9). This is of course not physical. In contrast, in the non-Markovian case, the tunneling coefficients and $\Delta_i(t)$ are time dependent and their initial values at the moment $t = 0$ when the QPC detector is brought to interact with the NMR are zero. Thus the individual contribution terms of the average current start from zero (see the blue solid lines in Fig. 9) and will approach their Markovian (finite-bandwidth) counterparts at a time scale of $\hbar/\Lambda_e$. The extra transient current term $I_{\{X,P\}}(t)$ of Eq. (86), plotted in Fig. 9(f), is proportional to the expectation value of the symmetrized product of the position and momentum operators of the NMR $\langle\{x, p\}(t)\rangle$ and thus oscillates with twice the frequency of ω_0. This additional term Eq. (86), which was generally ignored in the studies of the same problem in the literature,[19–23] has a coefficient proportional to the imaginary part of the combination of the QPC tunneling coefficients or bath correlation kernels (functions) of $\mathrm{Im}[\xi_1^a - \xi_2^a]$, where ξ_1^a and ξ_2^a are defined in Eqs. (44) and (46), respectively. Recall that the frequency renormalization $\tilde{\omega}_e^2(t)$ of Eq. (38) and the diffusion coefficient $h_e(t)$ of Eq. (41) are also proportional to the imaginary part of the QPC tunneling coefficients or bath correlation kernels (functions) but with different combinations. The value of the frequency normalization $\tilde{\omega}_e^2(t) \propto \mathrm{Im}[\xi_1^a(t) + \xi_2^a(t)]$ increases as Λ_e increases, and diverges as $\Lambda_e \to \infty$. So a counterterm is introduced for the purpose of frequency regularization. On the other hand, the value of the diffusion coefficient $h_e(t) \propto \mathrm{Im}[\xi_1^s(t) - \xi_2^s(t)]$ decreases as Λ_e increases even though the individual terms of the imaginary parts of $\xi_1^s(t)$ and $\xi_2^s(t)$ defined in Eqs. (43) and (45) diverge as $\Lambda_e \to \infty$. The typical values of $h_e(t)$ are however very small as compared to other time-dependent decoherence and dissipation coefficients (see Fig. 7) and thus $h_e(t)$ is often neglected. Similarly to $h_e(t)$, the extra transient current $I_{\{X,P\}}(t) \propto [\Delta_6(t) - \Delta_7(t)] \propto \mathrm{Im}[\xi_1^a(t) - \xi_2^a(t)]$ decreases as Λ_e increases even though the individual terms of the imaginary parts of $\xi_1^a(t)$ and $\xi_2^a(t)$ defined in Eqs. (44) and (46) also diverge as $\Lambda_e \to \infty$. However, $I_{\{X,P\}}(t)$ has a considerable magnitude and should be included into the time-dependent current. $I_{\{X,P\}}(t)$ is also proportional to $\langle\{x, p\}(t)\rangle$ which vanishes in the steady state, so $I_{\{X,P\}}(t)$ exists only in the transient regime. As mentioned, $I_{\{X,P\}}(t)$ decreases as Λ_e increases. Thus the contribution of $I_{\{X,P\}}(t)$ to the transient current is very small for large cutoff energies. Indeed, we can see from the red dashed line in Fig. 9(f) that $I_{\{X,P\}}(t)$ does not contribute to the transient current in the Markovian WBL case.

For clarity, we plot in Fig. 10(a) the difference between the total current and the isolated QPC tunneling current, i.e.,

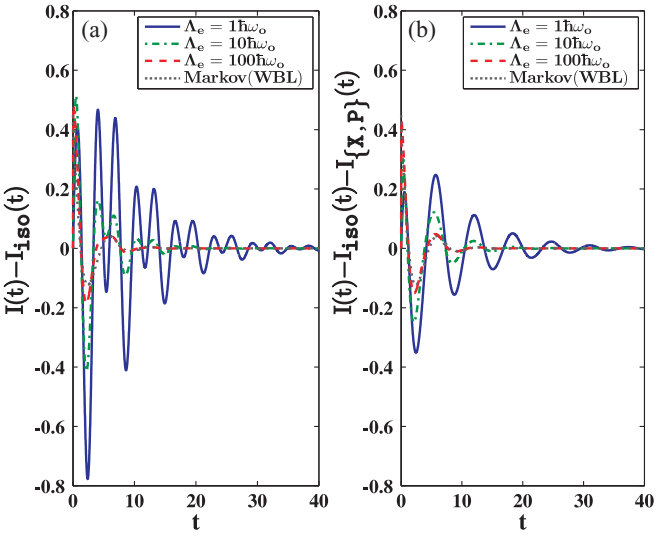

FIG. 10. (Color online) (a) Difference between the total current and the isolated QPC tunneling current, $I_{\mathrm{tot}}(t) - I_{\mathrm{iso}}(t)$, and (b) current in (a) with the contribution of $I_{\{X,P\}}(t)$ of Eq. (86) further deducted for different values of the Lorentzian cutoff energy: $(\Lambda_e/\hbar\omega_0) = 1$ (in blue solid lines), 10 (in red dashed lines), and 100 (in green dot-dashed lines). The Markovian WBL cases are plotted in gray dotted lines. The time-dependent average current is in units of $I_{\mathrm{iso}}^M = e^2VG_0$ and the time is in units of ω_0^{-1}. Other parameters used are $eV = 0.1\hbar\omega_0, k_BT = 0.1\hbar\omega_0, G_x x_0/G_0 = 0.04$, $G_p x_0/G_0 = 0.01, G_{xx}x_0^2/G_0 = 0.002$, and $\gamma_e^M = 0.12\omega_0$.

$I(t) - I_{\mathrm{iso}}(t)$, for different values of the cutoff energy. For comparison, we further deduct the contribution of $I_{\{X,P\}}(t)$ of Eq. (86) from $I(t) - I_{\mathrm{iso}}(t)$, and the resultant current is plotted in Fig. 10(b). In the steady state, the expectation values $\langle x\rangle_{t\to\infty} = \langle p\rangle_{t\to\infty} = \langle\{x, p\}\rangle_{t\to\infty} = 0$. Thus the total steady-state average current that approaches its Markovian long-time value becomes

$$I(t \to \infty) = I_{\mathrm{iso}}(t \to \infty) + I_{XX}(t \to \infty) + I_{QM}(t \to \infty). \tag{90}$$

It has been discussed in Ref. 21 that in the limit of small bias voltages and temperatures (i.e., $eV, k_BT \ll \hbar\omega_0$), the quantum correction current $I_{QM}(t \to \infty)$ in the steady state has to cancel $I_{XX}(t \to \infty)$ as the voltages and temperatures are too small to excite the NMR. As a result, the steady-state average current in this case is equal to that of an isolated QPC junction, $I_{\mathrm{iso}}(t \to \infty)$. This is indeed the case for the low values of voltage and temperature chosen in Figs. 9 and 10. We can see from Fig. 9(e) and the inset of Fig. 9(c) that the steady-state $I_{QM}(t \to \infty)$ does cancel the steady-state $I_{XX}(t \to \infty)$. As a result, the total average current difference $I(t) - I_{\mathrm{iso}}(t)$ in Fig. 10 vanishes in the steady state. We can also see from Figs. 10(a) and 10(b) that for a large cutoff energy or bandwidth of $\Lambda_e = 100\hbar\omega_0$, the evolution of the time-dependent current approaches that of the Markovian WBL case closely. Without including the contribution of $I_{\{X,P\}}(t)$ of Eq. (86) to the average current, there are still substantially quantitative differences between the Markovian WBL current and the non-Markovian currents with finite cutoff energies as shown in Fig. 10(b). Furthermore, significant qualitative and quantitative differences between the

non-Markovian currents and the Markovian WBL current in the short-time region are both clearly observed in Fig. 10(a). The non-Markovian transient currents with small values of cutoff energy are characterized by oscillations with large amplitudes and twice the NMR renormalized frequency as compared to the Markovian WBL one. We note that although a significant difference between the non-Markovian and Markovian WBL currents $I_{XX}(t)$ in Fig. 9(c) can be observed, the values of $I_{XX}(t)$ are small compared to those of the other individual current contribution terms. So this difference in $I_{XX}(t)$ may not be easily identified in the total average current as that of $I_{\{X,P\}}(t)$. This extra contribution of $I_{\{X,P\}}(t)$ of Eq. (86) was completely neglected in the discussion of the Markovian current for the same problem in the literature.[19–23] We find, however, that this extra significant contribution of $I_{\{X,P\}}(t)$ in the transient current may serve as a witness or signature of the non-Markovian features for the coupled NMR-QPC system with finite cutoff energies (bandwidths).

B. Inclusion of the effect of thermal bosonic environment

So far, we have not included the effect of the thermal bosonic environment in our numerical calculations. A natural question is whether including the effect of the bosonic environment changes the picture that the transient current can be used to witness non-Markovian effects of the coupled NMR-QPC system. Notice that most of the individual time-dependent current terms depend on the product of two factors: the combination of time-dependent coefficients $\Delta_i(t)$ and the time-dependent dynamical variables of the NMR. The inclusion of the effect of the thermal bosonic environment affects only the time evolution of the NMR dynamical variables but not the time-dependent coefficients $\Delta_i(t)$. So if the coupling of the NMR to the thermal environment is small compared with the coupling to the QPC reservoirs, then the main non-Markovian feature in the QPC transient current will remain. But if the coupling of the NMR to the thermal environment is comparable to the coupling to the QPC reservoirs, then the dynamical variables will reach their steady-state more quickly. Figure 11 shows the time evolutions of $\langle x(t)\rangle$, $\langle p(t)\rangle$, $\langle x^2(t)\rangle$, and $\langle\{x,p\}(t)\rangle$ for different values of the ratio of (γ_0^M/γ_e^M) that characterizes the coupling strength of the NMR-thermal bath relative to that of the NMR-QPC reservoirs. One can see in Fig. 11 that as the value of the ratio (γ_0^M/γ_e^M) increases for a fixed value of $\gamma_e^M = 0.12\omega_0$, the oscillation amplitudes of $\langle x(t)\rangle$, $\langle p(t)\rangle$, $\langle x^2(t)\rangle$, and $\langle\{x,p\}(t)\rangle$ diminish and the time at which the steady state is reached shifts to the short-time region since the total damping coefficient become larger. As a result, the differences in oscillation amplitudes between $I(t) - I_{\rm iso}(t)$ and $I(t) - I_{\rm iso}(t) - I_{\{X,P\}}(t)$ become small and the time intervals where the differences exist with characteristic oscillation frequency of $2\omega_0$ also become shorter(see Fig. 12). The oscillations will quickly reach their steady-state values and differences will become unobservable if the ratio of (γ_0^M/γ_e^M) becomes much larger than 1.

Another question is whether the case where there are no non-Markovian effects in the NMR-QPC system, but there are non-Markovian effects induced by the bosonic environment, will result in similar non-Markovian features in the transient current. The answer

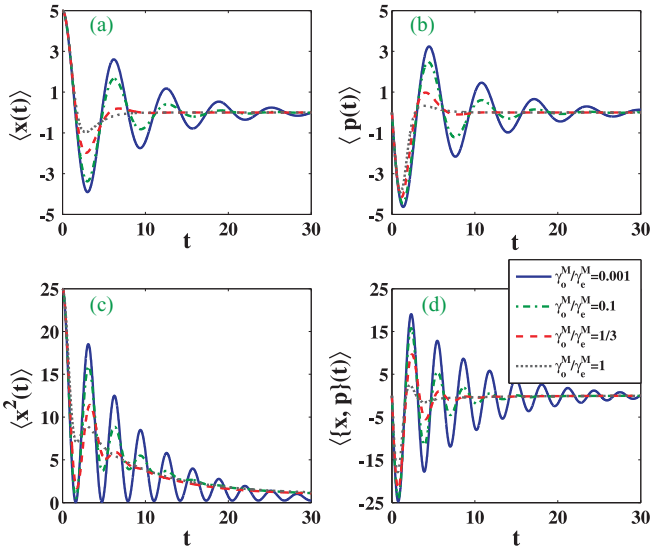

FIG. 11. (Color online) Time evolutions of the dynamical variables of the NMR (a) position $\langle x(t)\rangle$ in units of x_0, (b) momentum $\langle p(t)\rangle$ in units of p_0, (c) second-moment position $\langle x^2(t)\rangle$ in units of x_0^2, and (d) symmetrized second-moment position-momentum $\langle\{x,p\}(t)\rangle$ in units of x_0p_0 for different values of the ratio of $\gamma_0^M/\gamma_e^M = 0.001$ (in blue solid lines), 0.1 (in green dot-dashed lines), 1/3 (in red dashed lines), and 1 (in gray dotted line). The NMR is initially in a coherent state with $\langle x(0)\rangle = 5x_0$ and $\langle p(0)\rangle = 0$. The time is in units of ω_0^{-1}. Other parameters used are $eV = 0.1\hbar\omega_0$, $k_BT = 0.1\hbar\omega_0$, $\Lambda_e = \Lambda_0 = \hbar\omega_0$, and $\gamma_e^M = 0.12\omega_0$.

to the question can be found as follows. In our simple Lorentzian spectral density model, no non-Markovian

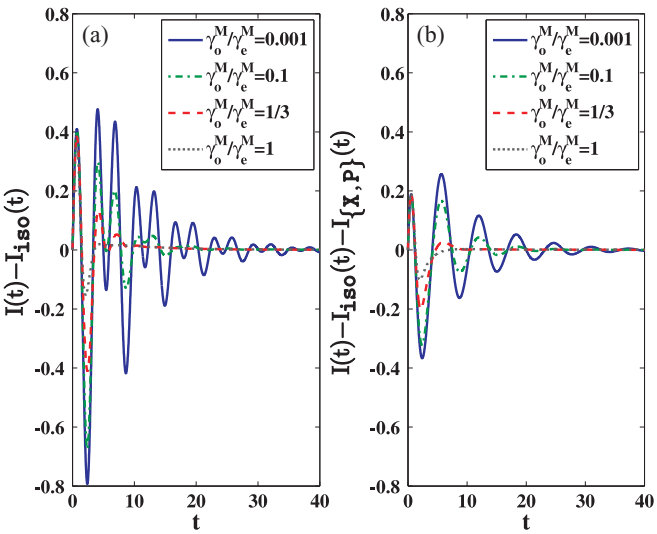

FIG. 12. (Color online) (a) Difference between the total current and the isolated QPC tunneling current, $I_{\rm tot}(t) - I_{\rm iso}(t)$, and (b) current in (a) with the contribution of $I_{\{X,P\}}(t)$ of Eq. (86) further deducted for different values of the ratio of $\gamma_0^M/\gamma_e^M = 0.001$ (in blue solid lines), 0.1 (in green dot-dashed lines), 1/3 (in red dashed lines), and 1 (in gray dotted lines). The time-dependent average current is in units of $I_{\rm iso}^M = e^2VG_0$ and the time is in units of ω_0^{-1}. Other parameters used are $eV = 0.1\hbar\omega_0$, $k_BT = 0.1\hbar\omega_0$, $\Lambda_e = \Lambda_0 = \hbar\omega_o$, $G_xx_0/G_0 = 0.04$, $G_px_0/G_0 = 0.01$, $G_{xx}x_0^2/G_0 = 0.002$, and $\gamma_e^M = 0.12\omega_0$.

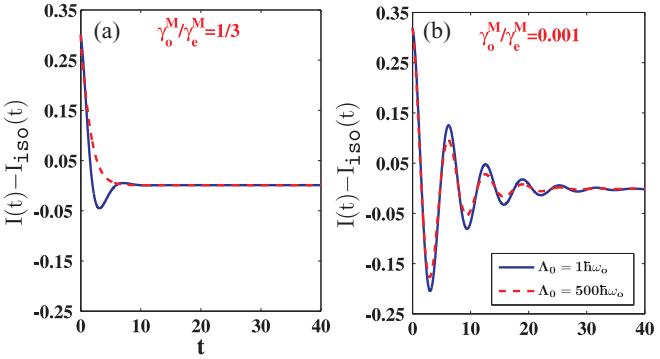

FIG. 13. (Color online) Current difference of $I(t) - I_{\rm iso}(t)$, for different values of the ratio of (a) $\gamma_0^M/\gamma_e^M = 1/3$ and (b) $\gamma_0^M/\gamma_e^M = 0.001$. The QPC reservoirs are in the WBL (i.e., $\Lambda_e \to \infty$), while the frequency bandwidth of the spectral density of the thermal bosonic bath is $\Lambda_0 = \omega_0$ (in blue solid lines) and $\Lambda_0 = 500\omega_0$ (in red dashed lines). The time-dependent average current is in units of $I_{\rm iso}^M = e^2 V G_0$ and the time is in units of ω_0^{-1}. Other parameters used are $eV = 0.1\hbar\omega_0$, $k_B T = 0.1\hbar\omega_0$, $G_x x_0/G_0 = 0.04$, $G_p x_0/G_0 = 0.01$, $G_{xx} x_0^2/G_0 = 0.002$, and $\gamma_e^M = 0.12\omega_0$.

effects in the NMR-QPC system implies that the cutoff energy or bandwidth of the QPC reservoir spectral density is very large (i.e., $\Lambda_e \gg \hbar\omega_0$ or in the WBL) since the Markovian limit can be justified by this condition. In the Markovian case, all the coefficients of $\Delta_i(t)$ become time independent. As mentioned previously, the time-dependent coefficient of $[\Delta_6 - \Delta_7] \propto {\rm Im}[\xi_1^a - \xi_2^a]$ of the extra transient current $I_{\{X,P\}}(t)$ decreases as Λ_e increases and becomes very small in the (Markovian) WBL. So $I_{\{X,P\}}(t)$ is very small in the Markovian WBL [see, e.g., Fig. 9(f)] even though $\langle\{x,p\}(t)\rangle$ has a considerable amplitude in the transient regime [see, e.g., Fig. 8(d)]. Therefore, if there are no non-Markovian effects in the NMR-QPC system (i.e., in the WBL), the extra transient current term $I_{\{x,p\}}(t)$ does not contribute even though there may still be significant oscillation amplitudes in $\langle\{x,p\}(t)\rangle$. Figure 13 shows the current difference of $I(t) - I_{\rm iso}(t)$ for different values of the ratio of (γ_o^M/γ_e^M) in the case where the QPC reservoirs are in the Markovian WBL (i.e., $\Lambda_e \to \infty$). The non-Markovian feature of oscillations with frequency of $2\omega_0$ in $I(t) - I_{\rm iso}(t)$ is unobservable in Fig. 13 as $I_{\{X,P\}}(t)$ does not contribute and $I_{XX}(t)$ is too small. The slight differences in $I(t) - I_{\rm iso}(t)$ between the cases of $\Lambda_0 = 1$ and $\Lambda_0 = 500$ are primarily due to the differences in $\langle x(t)\rangle$ and $\langle p(t)\rangle$ induced by the non-Markovian bosonic environment for the two different values of the spectral density frequency bandwidth Λ_0.

VIII. CONCLUSIONS

In summary, we have derived second-order time-local (time-convolutionless) non-Markovian conditional (n-resolved) and unconditional master equations of the reduced density matrix of a NMR subject to a measurement by a low-transparency QPC or tunnel junction detector and an influence by a thermal environment. Our non-Markovian master equations implemented with the reservoir memory correlation prescription going beyond the WBL allow us to study the memory effect of the nonequilibrium QPC fermionic reservoir and the equilibrium bosonic thermal bath on the NMR. Our non-Markovian master equations with time-dependent coefficients reduce, in appropriate limits, to various Markovian versions of master equations in the literature. Furthermore, our non-Markovian master equations are valid for arbitrary temperatures of the thermal environment and QPC reservoirs (detector), and for arbitrary bias voltages, as long as the perturbation theory up to the second order in the system-detector and system-environment coupling strength holds.

We have found considerable differences in dynamics between the non-Markovian cases and their Markovian counterparts. The facts that the QPC detector induces a back action on the NMR and the motion of the NMR modulates the current through the QPC are taken into account self-consistently. We have also calculated the time-dependent transport current through the QPC which contains information about the measured NMR system. We have found an extra transient current term of $I_{\{X,P\}}(t)$ of Eq. (86). This extra term, with a coefficient coming from the combination of the imaginary parts of the QPC reservoir correlation functions, was generally ignored in the studies of the same problem in the literature. But we find that it has a substantial contribution to the total transient current in the non-Markovian finite-bandwidth case and differs qualitatively and quantitatively from its Markovian WBL counterpart. Thus it may serve as a witness or signature of non-Markovian features for the coupled NMR-QPC system.

ACKNOWLEDGMENTS

We would like to acknowledge support from the National Science Council, Taiwan, under Grant No. 97-2112-M-002-012-MY3, support from the Frontier and Innovative Research Program of the National Taiwan University under Grants No. 99R80869 and No. 99R80871, and support from the focus group program of the National Center for Theoretical Sciences, Taiwan. We are grateful to the National Center for High-Performance Computing, Taiwan, for computer time and facilities.

*Corresponding author; goan@phys.ntu.edu.tw

[1] H. G. Graighead, Science **290**, 1532 (2000).
[2] M. Roukes, Phys. World **14**, 25 (2001).
[3] M. Blencowe, Phys. Rep. **395**, 159 (2004).
[4] D. H. Santamore, H.-S. Goan, G. J. Milburn, and M. L. Roukes, Phys. Rev. A **70**, 052105 (2004).
[5] W. K. Hensinger, D. W. Utami, H.-S. Goan, K. Schwab, C. Monroe, and G. J. Milburn, Phys. Rev. A **72**, 041405 (2005).
[6] L. F. Wei, Y.-X. Liu, C. P. Sun, and F. Nori, Phys. Rev. Lett. **97**, 237201 (2006).
[7] C. P. Sun, L. F. Wei, Y.-X. Liu, and F. Nori, Phys. Rev. A **73**, 022318 (2006).
[8] L. Y. Gorelik, A. Isacsson, M. V. Voinova, B. Kasemo, R. I. Shekhter, and M. Jonson, Phys. Rev. Lett. **80**, 4526 (1998); N. M Chtchelkatchev, W. Belzig, and C. Bruder, Phys. Rev. B **70**, 193305 (2004); D. Fedorets, L. Y. Gorelik, R. I. Shekhter, and M. Jonson, Phys. Rev. Lett. **92**, 166801 (2004).

[9] H. Park, J. Park, A. K. L. Lim, E. H Anderson, A. P. Alivisatos, and P. L McEuen, Nature (London) **407**, 57 (2000); A. Erbe, C. Weiss, W. Zwerger, and R. H. Blick, Phys. Rev. Lett. **87**, 096106 (2001).

[10] D. W. Utami, H.-S. Goan, and G. J. Milburn, Phys. Rev. B **70**, 075303 (2004); D. W. Utami, H.-S. Goan, C. A. Holmes, and G. J. Milburn, *ibid.* **74**, 014303 (2006); J. Twamley, D. W. Utami, H.-S. Goan, and G. Milburn, New J. Phys. **8**, 63 (2006).

[11] S. H. Ouyang, J. Q. You, and F. Nori, Phys. Rev. B **79**, 075304 (2009).

[12] M. P. Blencowe and M. N. Wybourne, Appl. Phys. Lett. **77**, 3845 (2000); Y. Zhang and M. P. Blencowe, J. Appl. Phys. **91**, 4249 (2002); R. Knobel and A. N. Cleland, Appl. Phys. Lett. **81**, 2258 (2002).

[13] R. G. Knobel and A. N. Cleland, Nature (London) **424**, 291 (2003).

[14] M. LaHaye *et al.*, Science **304**, 74 (2003).

[15] A. Naik, O. Buu, M. D. LaHaye, A. D. Armour, A. A. Clerk, M. P. Blencowe, and K. C. Schwab, Nature (London) **443**, 193 (2006).

[16] M. Poggio, M. P. Jura, C. L. Degen, M. A. Topinka, H. J. Mamin, D. Goldhaber-Gordon, and D. Rugar, Nature Phys. **4**, 635 (2008).

[17] D. A. Rodrigues and A. D. Armour, New J. Phys. **7**, 251 (2005); A. D. Armour, M. P. Blencowe, and Y. Zhang, Phys. Rev. B **69**, 125313 (2004); A. D. Armour, *ibid.* **70**, 165315 (2004).

[18] D. Mozyrsky, I. Martin, and M. B. Hastings, Phys. Rev. Lett. **92**, 018303 (2004).

[19] D. Mozyrsky and I. Martin, Phys. Rev. Lett. **89**, 018301 (2002).

[20] A. A. Clerk and S. M. Girvin, Phys. Rev. B **70**, 121303(R) (2004).

[21] J. Wabnig, D. V. Khomitsky, J. Rammer, and A. L. Shelankov, Phys. Rev. B **72**, 165347 (2005).

[22] A. Y. Smirnov, L. G. Mourokh and N. J. M. Horing, Phys. Rev. B **67**, 115312 (2003).

[23] J. Wabnig, J. Rammer, and A. L. Shelankov, Phys. Rev. B **75**, 205319 (2007).

[24] A. Shnirman and G. Schön, Phys. Rev. B **57**, 15400 (1998); Y. Makhlin, G. Schön, and A. Shnirman, Rev. Mod. Phys. **73**, 357 (2001).

[25] H.-S. Goan, Phys. Rev. B **70**, 075305 (2004).

[26] S. A. Gurvitz, Phys. Rev. B **56**, 15215 (1997); S. A. Gurvitz and Ya. S. Prager, *ibid.* **53**, 15932 (1996); S. A. Gurvitz, L. Fedichkin, D. Mozyrsky, and G. P. Berman, Phys. Rev. Lett. **91**, 066801 (2003).

[27] A. N. Korotkov, Phys. Rev. B **60**, 5737 (1999); **63**, 115403 (2001).

[28] H.-S. Goan, G. J. Milburn, H. M. Wiseman, and H. B. Sun, Phys. Rev. B **63**, 125326 (2001); H.-S. Goan and G. J. Milburn, *ibid.* **64**, 235307 (2001).

[29] H.-S. Goan, Quantum Inf. Comput. **3**, 121 (2003).

[30] T. M. Stace and S. D. Barrett, Phys. Rev. Lett. **92**, 136802 (2004).

[31] X. Q. Li, W. K. Zhang, P. Cui, J. Shao, Z. Ma, and Y. J. Yan, Phys. Rev. B **69**, 085315 (2004).

[32] X. Q. Li, P. Cui, and Y. J. Yan, Phys. Rev. Lett. **94**, 066803 (2005); X. Q. Li, J. Luo, Y. G. Yang, P. Cui, and Y. J. Yan, Phys. Rev. B **71**, 205304 (2005); X. Q. Li and Y. J. Yan, *ibid.* **75**, 075114 (2007).

[33] M. T. Lee and W. M. Zhang, J. Chem. Phys. **129**, 224106 (2008).

[34] W. Lu, Z. Ji, L. Pfeiffer, K. W. West, and A. J. Rimberg, Nature (London) **423**, 422 (2003); T. Fujisawa, T. Hayashi, Y. Hirayama, H. D. Cheong, and Y. H. Jeong, Appl. Phys. Lett. **84**, 2343 (2004); J. Bylander, T. Duty, and P. Delsing, Nature (London) **434**, 361 (2005); J. M. Elzerman, R. Hanson, L. H. Willems van Beveren, B. Witkamp, L. M. V. Vandersypen, and L. P. Kouwenhoven, *ibid.* **430**, 431 (2004); S. Gustavsson, R. Leturcq, B. Simovic, R. Schleser, T. Ihn, P. Studerus, K. Ensslin, D. C. Driscoll, and A. C. Gossard, Phys. Rev. Lett. **96**, 076605 (2006); S. Gustavsson, R. Leturcq, M. Studer, I. Shorubalko, T. Ihn, K. Ensslin, D. C. Driscoll, and A. C. Gossard, Surf. Sci. Rep. **64**, 191 (2009).

[35] T. Kwapiński, R. Taranko, and E. Taranko, Phys. Rev. B **66**, 035315 (2002).

[36] Y. Zhu, J. Maciejko, T. Ji, H. Guo, and J. Wang, Phys. Rev. B **71**, 075317 (2005).

[37] J. Maciejko, J. Wang, and H. Guo, Phys. Rev. B **74**, 085324 (2006).

[38] Z. Feng, J. Maciejko, J. Wang, and H. Guo, Phys. Rev. B **77**, 075302 (2008).

[39] S. Welack, M. Schreiber, and U. Kleinekathofer, J. Chem. Phys. **124**, 044712 (2006).

[40] D. Hou, Y. He, X. Liu, J. Kang, J. Chen, and R. Han, Physica E (Amsterdam) **31**, 191 (2006).

[41] J. Jin, M. W. Y. Tu, W. M. Zhang, and Y. Yan, New J. Phys. **12**, 083013 (2010); X. Zheng, J. Luo, J. Jin, and Y. Yan, J. Chem. Phys. **130**, 124508 (2009).

[42] M. W. Y. Tui and W. M. Zhang, Phys. Rev. B **78**, 235311 (2008).

[43] U. Kleinekathöfer, J. Chem. Phys. **121**, 2505 (2004).

[44] P. Zedler, G. Schaller, G. Kiesslich, C. Emary, and T. Brandes, Phys. Rev. B **80**, 045309 (2009).

[45] F. Shibata, Y. Takahashi, and N. Hashitsume, J. Stat. Phys. **17**, 171 (1977); S. Chaturvedi and F. Shibata, Z. Phys. B **35**, 297 (1979).

[46] H. P. Breuer, B. Kappler, and F. Petruccione, Phys. Rev. A **59**, 1633 (1999); Ann. Phys. (NY) **291**, 36 (2001).

[47] M. Schröder, U. Kleinekathöfer, and M. Schreiber, J. Chem. Phys. **124**, 084903 (2006).

[48] H. P. Breuer and F. Petruccione, *The Theory of Open Quantum Systems* (Oxford University Press, Oxford, 2002); S. T. Barnett and P. M. Radmore, *Methods in Theoretical Quantum Optics* (Clarendon Press, Oxford, 2002).

[49] J. P. Paz and W. H. Zurek, in *Coherent Matter Waves*, edited by R. Kaiser, C. Westbrook, and F. David, *Proceedings of the Les Houches Summer School, LXXII* (Springer-Verlag, Berlin, 2001).

[50] K.-L. Liu and H.-S. Goan, Phys. Rev. A **76**, 022312 (2007).

[51] E. Ferraro, M. Scala, R. Migliore, and A. Napoli, Phys. Rev. A **80**, 042112 (2009).

[52] Sinayskiy *et al.*, J. Phys. A **42**, 485301 (2009).

[53] D. Mogilevtsev *et al.*, J. Phys. Condens. Matter **21**, 055801 (2009).

[54] P. Haikka and S. Maniscalco, Phys. Rev. A **81**, 052103 (2010); P. Haikka, e-print arXiv:0911.4600.

[55] Md. M. Ali, P.-W. Chen, and H.-S. Goan, Phys. Rev. A **82**, 022103 (2010).

[56] W. T. Strunz and T. Yu, Phys. Rev. A **69**, 052115 (2004).

[57] F. Haake and R. Reibold, Phys. Rev. A **32**, 2462 (1985).

[58] B. L. Hu, J. P. Paz, and Y. Zhang, Phys. Rev. D **45**, 2843 (1992).

[59] M. G. Palma, K.-A. Suominen, and A. Ekert, Proc. R. Soc. London, Ser. A **452**, 567 (1996).

[60] L.-M. Duan and G.-C. Guo, Phys. Rev. A **57**, 737 (1998).

[61] L. Diósi, N. Gisin, and W. T. Strunz, Phys. Rev. A **58**, 1699 (1998).

[62] John H. Reina, Luis Quiroga, and Neil F. Johnson, Phys. Rev. A **65**, 032326 (2002).

[63] G. Schaller and T. Brandes, Phys. Rev. A **78**, 022106 (2008).

[64] H.-S. Goan, C.-C. Jian, and P.-W. Chen, Phys. Rev. A **82**, 012111 (2010).

[65] H. J. Carmichael, *Statistical Methods in Quantum Optics 1* (Springer, Berlin, 1999).

[66]S. T. Barnett and P. M. Radmore, *Methods in Theoretical Quantum Optics* (Clarendon Press, Oxford, 2002).
[67]M. M. Wolf, J. Eisert, T. S. Cubitt, and J. I. Cirac, Phys. Rev. Lett. **101**, 150402 (2008).
[68]H. P. Breuer, E. M. Laine, and J. Piilo, Phys. Rev. Lett. **103**, 210401 (2009).
[69]A. Rivas, S. F. Huelga, and M. B. Plenio, Phys. Rev. Lett. **105**, 050403 (2010).
[70]X. M. Lu, X. Wang, and C. P. Sun, Phys. Rev. A **8**, 042103 (2010).
[71]C. Fleming, N. I. Cummings, C. Anastopoulos, and B. L. Hu, e-print arXiv:1003.1749.
[72]S. Maniscalco, J. Piilo, F. Intravaia, F. Petruccione, and A. Messina, Phys. Rev. A **70**, 032113 (2004).
[73]F. Intravaia, S. Maniscalco, and A. Messina, Phys. Rev. A **67**, 042108 (2003).
[74]N. S. Wingreen and Y. Meir, Phys. Rev. B **49**, 11040 (1994).
[75]T. S. Ho, S. H. Hung, H. T. Chen, and S.-I. Chu, Phys. Rev. B **79**, 235323 (2009).
[76]In the proofreading stage, we find that an extra term of $-(i/\hbar)Q_e(t)[x,\rho_R(t)]$ should appear in Eq. (37), where the coefficient $Q_e(t) = -(\hbar\, G_p/\pi)\mathrm{Re}[\xi_3^a(t)] - (\hbar\, G_x/\pi)\mathrm{Im}[\xi_3^a(t)]$. Here $\xi_3^a(t) = f_F^+(t,eV) - f_B^+(t,-eV)$ with $f_F^+(t,eV)$ and $f_B^+(t,-eV)$ defined respectively in Eqs. (24) and (25), and G_x and G_p are defined in the text below Eq. (75) and Eq. (79), respectively. However, the coefficient $Q_e(t)$ diverges as the cutoff energy $\Lambda_e \to \infty$. Thus an counterterm similar to that of the frequency renormalization (regularization) discussed in the text below Eq. (47) should be added to compensate the contribution of $Q_e(t \to \infty)$ at large time. Because of the existence of this term, the equations of motion of NMR dynamical variables of Eqs. (62)–(67) should be slightly modified. But we find that the contributions from this regularized extra term make almost no difference in the time evolutions of the NMR dynamical variables and the time evolutions of the currents for the large Λ_e cases, and make only tiny difference for the small Λ_e cases. Thus the description and the main conclusion of this paper remain unchanged.
[77]L. H. Ryder, *Quantum Field Theory*, 2nd ed. (Cambridge University Press, Cambridge, 1996).
[78]F. Mandl and G. Shaw, *Quantum Field Theory*, rev. ed. (John Wiley & Son, Chichester, 1993).
[79]A. Săndulescu, H. Scutaru, and W. Scheid, Ann. Phys. (NY) **173**, 277 (1987).
[80]J. Rammer, A. L. Shelankov, and J. Wabnig, Phys. Rev. B **70**, 115327 (2004).